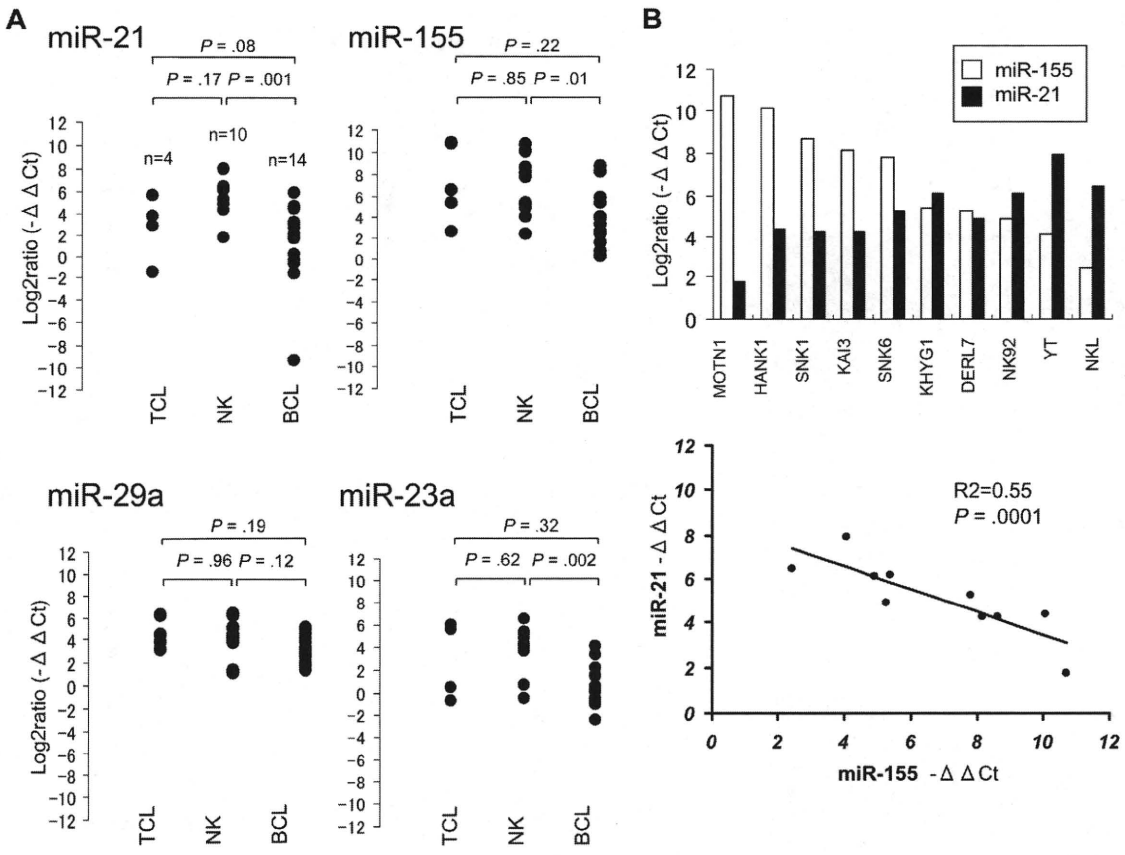

Figure 2. Comparison of miRNA expression in T-, B-, and NK-cell lymphoma/leukemia lines with quantitative RQ-PCR (Taqman PCR). (A) Taqman PCR analysis of miR-21, miR-23a, miR-29a, and miR-155 expression in 4 T-cell, 10 NK-cell, and 14 B-cell lymphoma/leukemia lines. The significance of differences between T- and NK-cell, between NK- and B-cell, and between T- and B-cell lymphoma/leukemia lines were assessed by use of the Student *t* test. The following B- and T-cell lymphoma/leukemia lines were used for this study. SUDHL4, SUDHL6, OCI-Ly3, and OCI-Ly7 cells were derived from diffuse large B-cell lymphoma; Raji, Daudi, Ramous, Namalwa, and D.G-75 cells were derived from Burkitt lymphoma; SP-49 and Jeko-1 cells were derived from mantle cell lymphoma; FL-18 cells were derived from follicular lymphoma; Karpass 1718 and SLVL cells were derived from splenic virus lymphoma; ATN1 cells were derived from adult T-cell leukemia; JM and MOLT4 cells were derived from T-cell leukemia; and MyLa cells were derived from peripheral T-cell lymphoma unspecified. (B) Correlation between expression miR-21 and miR-155 in 10 NK-cell lymphoma/leukemia lines. In the top panel, □ and ■ bars depict $-\Delta\Delta C_t$ values for miR-155 and miR-21 expression, respectively. In the bottom panel: y-axis, $-\Delta\Delta C_t$ values for miR-21 expression; x-axis, $-\Delta\Delta C_t$ values for miR-155 expression are shown. The *P* value was calculated by simple regression analysis.

these microRNAs are associated with NK-cell lymphomagenesis, we examined the effects of antisense oligonucleotides targeted to miR-21 (ASO-21) and miR-155 (ASO-155) in NK-cell lymphoma/leukemia lines, which constitutively overexpress miR-21 but show very little expression of miR-155. Northern analysis revealed no expression of miR-21 in NKL cells treated with ASO-21 compared with cells treated with scrambled control oligonucleotide (SCO-21). To investigate effects of ASO assay, we performed apoptosis and cell assays. We found that ASO-21 increased the incidence of apoptosis among NKL cells exposed to 100 μmol/L etoposide for 4 hours (Figure 4A). When we performed a cell-cycle analysis of ASO-21–treated NKL cells, we detected no significant differences in the respective cell-cycle stages between SCO-21–treated and ASO-21–treated cells (Figure 4B). Because Apaf-1, RECK, PDCD4, Spry1, Spry2, and PTEN are all candidate targets of miR-21 in tumorigenesis,[19-23] we next conducted Western analyses with cells treated with SCO-21 and ASO-21 (Figure 4C). We found that among these candidate targets, PTEN and PDCD4 were up-regulated in ASO-21–treated cells compared with SCO-21–treated cells. Moreover, we found that levels of activated AKT (pAKT), a downstream target in the PTEN/AKT signaling pathway, were reduced, whereas those of the proapoptotic protein Bim, a downstream target of pAKT via FoxO3, were increased.[24,25] Western analysis of p21 levels in SCO-21– and ASO-21–treated NKL cells revealed no expression of p21 but a slight increase in p53 levels in ASO-21–treated cells. There was no difference in the levels of p27 expression between SCO- and ASO-treated cells. To confirm the function of miR-21, we examined the effects ASO-21 in YT cells, which overexpress miR-21 with little expression of miR-155. As with NKL cells, cell-cycle analysis showed no difference between SCO-21–treated and ASO-21–treated YT cells (data not shown). By contrast, ASO-21 enhanced apoptotic activity in YT cells after exposure to 100 μmol/L etoposide (Figure 4E). YT cells treated with ASO-21 also showed up-regulation of PTEN and down-regulation of pAKT, as was seen in NKL cells (Figure 4E). These results suggest that miR-21 contributes to NK-cell lymphomagenesis by reducing apoptotic activity but not cell-cycle progression.

Because MOTN1 cells showed less expression of miR-21 than the other NK-cell lymphoma cell lines, we transduced these cells by using a lentiviral vector encoding both miR-21 and GFP, which yielded greater than 95% GFP positivity. Subsequent Taqman PCR analysis showed that miR-21 expression was 2.6-fold greater in the transduced MOTN1 cells than in control cells. As with the other cells tested, we detected no difference in the respective cell-cycle stages between control cells and miR-21 transductants (data not shown). However, apoptotic activity was diminished in MOTN1 cells transduced with miR-21 (Figure 4F), whereas Western analysis showed that levels of PTEN and PDCD4

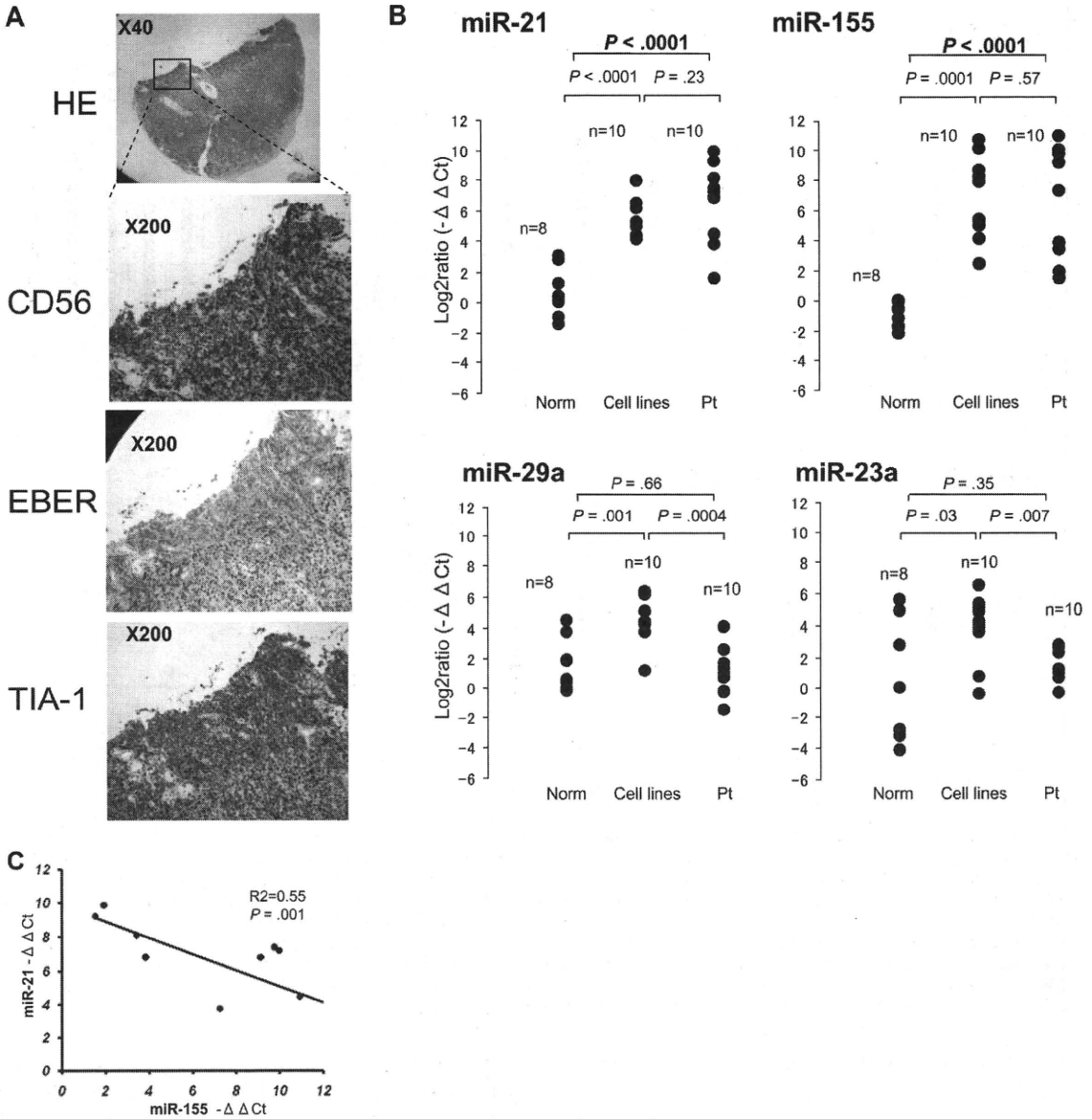

Figure 3. Quantitative PCR analysis of miRNA levels in specimens of primary NK-cell lymphoma/leukemia. (A) Histopathologic features of a typical specimen of primary extranodal NK/T-cell lymphoma, nasal type (NKpt5). Hematoxylin and eosin–stained (×40), CD56-stained, EBER-ISH–stained, and TIA-1-stained (×200) cells are shown. (B) Quantitative PCR analysis of mature miR-21, miR-23a, miR-29a, and miR-155 in normal $sCD3^-CD56^+$ cells (n = 8), NK-cell lymphoma/leukemia lines (n = 10), and specimens of primary NK-cell lymphoma/leukemia (n = 10). Y-axis: $-\Delta\Delta C_t$ values for miRNA expression. The significance of differences between groups was evaluated by the use of the Student *t* test. (C) Correlation between miR-21 and miR-155 expression in 10 primary lymphoma/leukemia specimens. y-axis, $-\Delta\Delta C_t$ values of miR-21 expression; x-axis, $-\Delta\Delta C_t$ values miR-155 expression. The *P* value was calculated by simple regression analysis.

were reduced and those of pAKT were increased in the transductant cells (Figure 4F). Total AKT levels were unaffected by miR-21. Collectively, these findings suggest miR-21 acts as an oncomiRNA through dysregulation of the PTEN/AKT signaling pathway, resulting in diminished apoptotic activity.

miR-155 induces dysregulation of SHIP1/AKT signaling in NK-cell lymphomas/leukemias

We next used ASO-155 to examine the effects of reducing miR-155 expression in SNK6 and MOTN1 cells, both of which overexpress miR-155 (Figure 5A). By using Target Scan software,[21] we determined that one likely target of miR-155 is SHIP1, an inositol 5-phosphatase expressed in hemopoietic cells. By hydrolyzing the 5-phosphates from PtdIns(3,4,5)P(3) and Ins(1,3,4,5)P,(4), SHIP1 negatively regulates signaling in the phosphoinositide 3-kinase (PI3K)–AKT pathway. Consequently, inhibition of SHIP1expression by miR-155 would likely increase activity in the AKT pathway.

Western analysis revealed that treating SNK6 and MOTN1 with ASO-155 increased expression of SHIP1 (Figure 5B) and reduced levels of pAKT in both cell lines. Interestingly, MOTN1 cells treated with ASO-155 showed greater levels of p21 and p27 than SCO-treated cells. ASO-155–treated SNK6 cells also showed greater levels of SHIP1 and lower levels of pAKT, but unlike MOTN1 cells they did not show up-regulation of p21. This finding may reflect the fact that, in MOTN1 cells, p21 expression is regulated by SHIP1/AKT signaling and is unaffected by p53, whereas in SNK6 cells p21 expression can be regulated by wild-type p53. It thus appears that continuous overexpression of miR-155 leads to increased production of pAKT via down-regulation of SHIP1. It is noteworthy that transduction of MOTN1

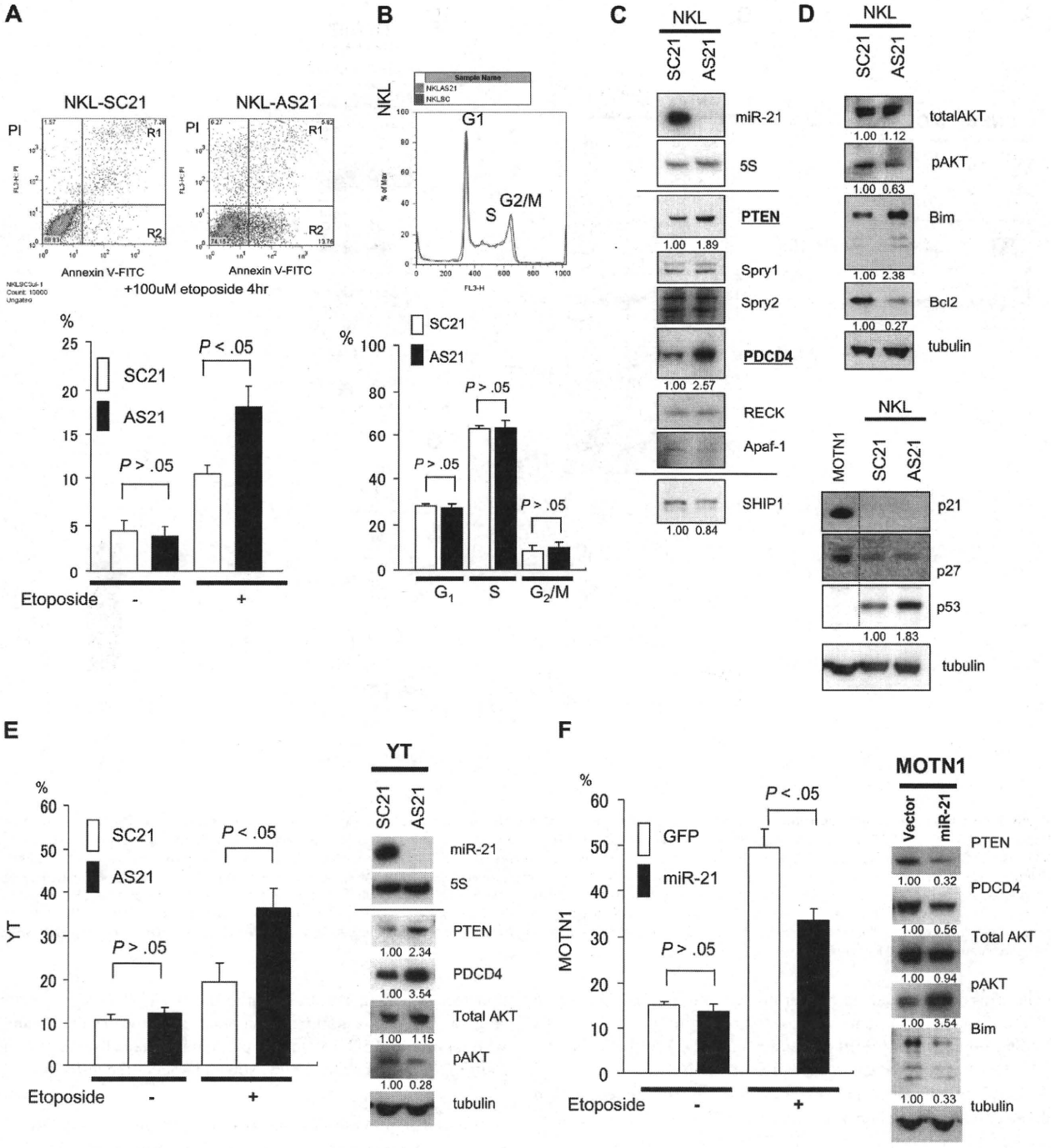

Figure 4. Targets of miR-21 and the function in NK-cell lymphoma/leukemia. (A) Apoptosis among NKL cells. ASO-21– and SCO-21–treated cells were exposed to 100 μmol/L etoposide for 4 hours. Top panels show flow cytometric analysis of ASO-21–treated and SCO-21–treated NKL cells: y-axis, cells stained by propidium iodide (PI); x-axis, cells stained by annexin V–FITC. Apoptotic cells are in Regions 1 (R1) and 2 (R2). Apoptotic (R1 + R2) cells of ASO-21–treated cells are showing significantly greater percentages than those cells treated with SCO-21. Bottom panel shows the percentages of apoptotic cells (R1 + R2). □ and ■ depict percent apoptosis (R1 + R2) among NKL cells treated with SCO-21 and ASO-21, respectively. Symbols and bars indicate means and SDs of triplicate samples. (B) Cell-cycle analysis for NKL cells treated with ASO-21 or SCO-21. In the top panel, red lines show the cell-cycle pattern of cells treated with SCO-21, whereas green lines show the cell-cycle pattern of those treated with ASO-21. G_1, S, and G_2/M phases are shown as described. Average (n = 3) percentages among SCO-treated NKL cells: G_1, 29.3%; S, 61.3%; and G_2/M, 9.4%. Average (n = 3) percentages among ASO-treated NKL cells: G_1, 25.3%; S, 66.5%; and G_2/M, 8.2%. (C) Western analysis for direct candidate targets of miR-21 of NKL cell line treated with ASO-21 and SCO-21. Northern blot analysis of miR-21 in NKL cells treated with ASO-21 and SCO-21 are also shown. Fold changes in proteins expression are shown below the gels and normalized to the level in NKL SCO-21 treated cells, which are assigned a value of 1.00. (D) Western analysis for candidate downstream targets of miR-21 of NKL cell line treated with ASO-21 and SCO-21. Fold changes in proteins expression are shown below the gels and normalized to the level in NKL SCO-21–treated cells, which are assigned a value of 1.00. Bottom panel shows an immunoblot analysis of p21, p27, and p53 in NKL cells treated with ASO-21 or SCO-21. (E) Incidence of apoptosis among YT cells. In the left panel, cells treated with ASO-21 or SCO-21 were exposed to 100 μmol/L etoposide for 4 hours. □ and ■ depict percent apoptosis among YT cells treated with SCO-21 and ASO-21, respectively. Symbols and bars indicate means and SDs of triplicate samples. Apoptotic cells of ASO-21–treated cells show significantly greater percentages than those cells treated with SCO-21. In the right panel, Western analysis of miR-21 targets in YT cells treated with ASO-21 or SCO-21. Fold changes in protein expression are shown below the gels and normalized to the level in SCO-21–treated cells, which was assigned a value of 1.00. (F) Incidence of apoptosis among transduced MOTN1 and control cells. In the left panel, MOTN1 cells transduced with miR-21 plus GFP or GFP alone (control) were exposed to 100 μmol/L etoposide for 4 hours. □ and ■ depict percent apoptosis among GFP-transduced (control) and miR-21–transduced cells, respectively. Symbols and bars indicate means and SDs of triplicate samples. Apoptotic cells of miR-21 transduced cells show significantly lower percentages than those of control cells. In the right panel, Western analysis of PTEN, pAKT, total AKT, and Bim expression in MOTN1 cells. Fold changes in protein expression are shown below the gels and are normalized to the level in GFP-transduced control cells, which was assigned a value of 1.00.

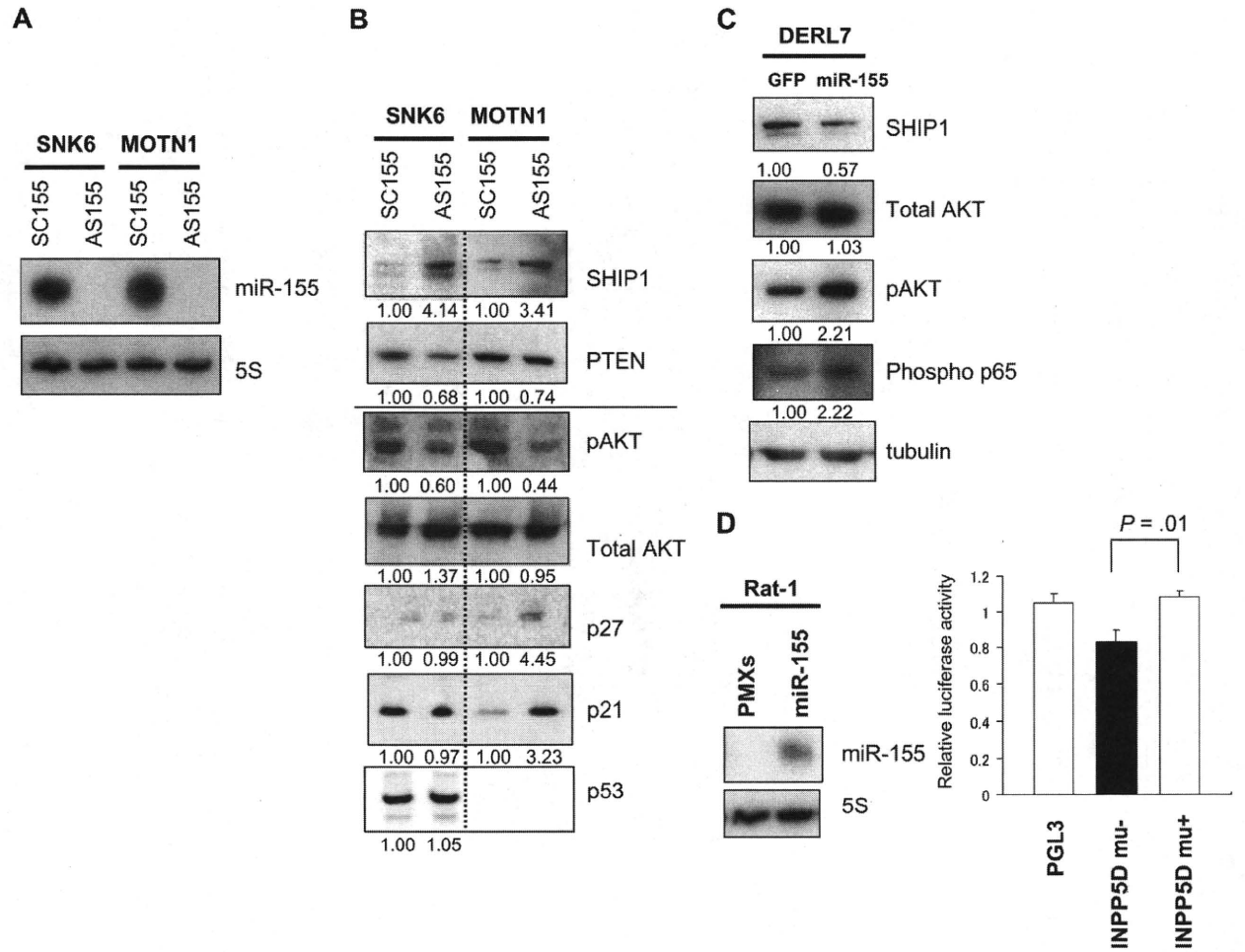

Figure 5. miR-155 induces dysregulation of SHIP1 signaling to AKT in NK-cell lymphoma/leukemia lines. (A) Northern analysis of miR-155 in SNK6 and MOTN1 cells treated with ASO-155 or SCO-155. Controls (5S tRNA) are shown below the miR-155 blots. (B) Western analysis of PTEN, pAKT, total AKT, p21, p27, and p53 expression in MOTN1 and SNK6 cells treated with ASO-155 or SCO-155. Fold changes in protein expressions are shown below the gels and are normalized to the levels in SCO-treated SNK6 or MOTN1 cells, respectively, which were assigned a value of 1.00. (C) Western analysis of SHIP1, total AKT, pAKT, and phospho-NFκB (Phospho p65) in DERL7 cells transduced with miR-155 plus GFP or GFP alone (control). Fold changes in protein expression are shown below the gels and are normalized to the level in the GFP-transduced control cells, which was assigned a value of 1.00. (D) Luciferase reporter assay of *INPP5D/SHIP* expression in Rat-1 cells transfected with miR-155 (PMXs-miR-155-puro) or empty vector (PMXs-puro). Blots showing MiR-155 expression are beside the bars. The significance of differences between wild-type pGL3-*INPP5D* 3′UTR and pGL3-*INPP5D* was evaluated with the Student *t* test.

cells with miR-21 leads to further up-regulation of pAKT (Figure 4F) in the context of continuous overexpression of miR-155. This finding suggests that forced expression of miR-21 further enhances pAKT expression via down-regulation of PTEN.

Levels of miR-155 expression were lower in DERL7 cells than in the other NK-cell lymphoma lines tested (Figure 1A) but were increased 3.1-fold by transduction with miR-155 using a lentiviral vector. This increase in miR-155 expression led to down-regulation of SHIP1 and up-regulation of pAKT (Figure 5C). Moreover, immunoblotting of downstream targets of AKT, including Bim, p21, p27, and phosphorylated NF-κB (phospho-p65), revealed that levels of phospho-p65 were increased in the miR-155 transductants, which suggests NF-κB activation via pAKT may also contribute to lymphomagenesis.

To determine whether expression of *INPP5D/SHIP*, which encodes SHIP1, is directly regulated by miR-155, we performed luciferase reporter assays by using Rat-1 fibroblasts stably expressing miR-155. Rat-1 fibroblast stably expressing miR-155 was established by retrovirus transduction with PMXs-premiR-155-puromycine vector. We found that when the cells were transfected with a reporter construct harboring wild-type *INPP5D/SHIP*, luciferase activity was significantly repressed compared with cells transfected with a construct harboring a *INPP5D/SHIP* mutant (Figure 5D). These findings, combined with the results obtained with the use of ASO-155 in NK-cell lymphoma cells, suggest that *INPP5D/SHIP1* is a direct downstream target of the miR-155.

Antisense oligonucleotide assay of miR-21 and miR-155 for a KAI3, which is overexpressing the microRNAs, showed dysregulation of PTEN/AKT and SHIP1/AKT signaling

KAI3 cells overexpress both miR-21 and miR-155 (Figures 1-3). When we treated these cells with ASO-21 or ASO-155, we detected no change in the expression of pAKT. However, when we treated the cells with a combination of ASO-21 and ASO-155, which reduced expression of both miR-21 and miR-155 (Figure 6A), levels of PTEN and SHIP1 were increased (Figure 6B), and those of pAKT were reduced. The incidences of apoptotic and necrotic cells among ASO-21/155–treated cells were greater than among SCO-treated cells, which suggests that reducing expression of miR-21 and miR-155 enhances apoptotic activity in KAI3 cells (Figure 6C). In addition, up-regulation PDCD4 was also detected (Figure 6B). Thus miR-21 and miR-155 may act in concert to enhance

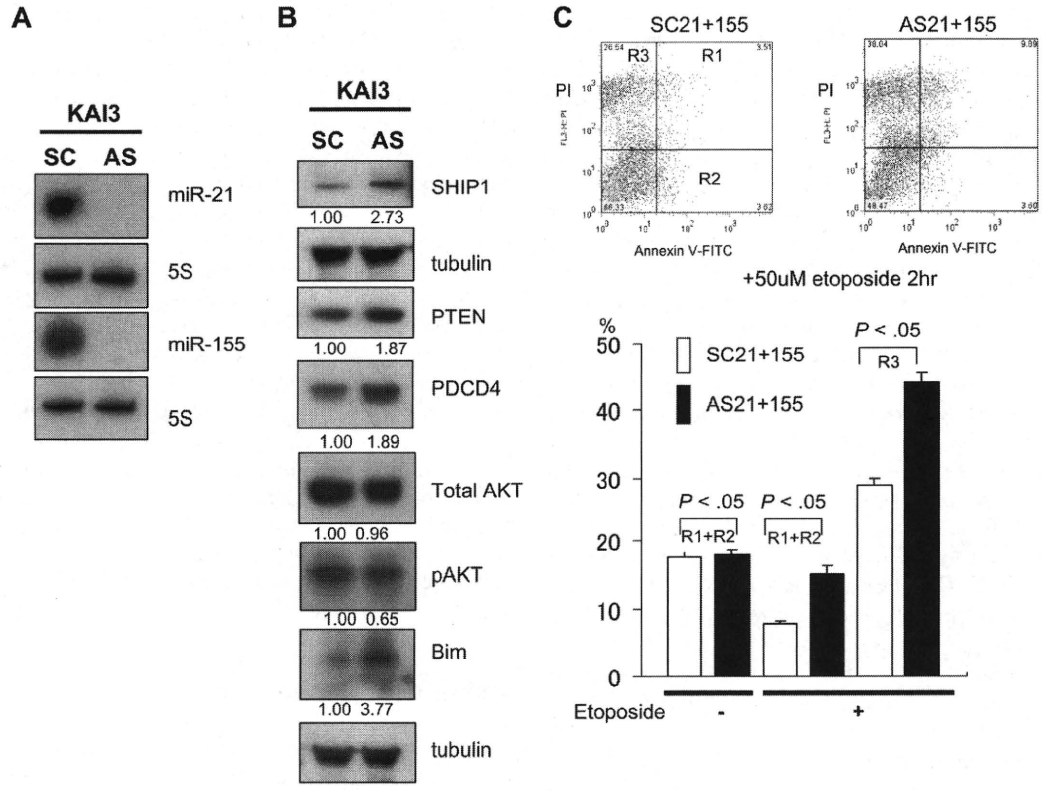

Figure 6. Effects of ASO-21 and ASO-155 in KAI3 cells. (A) Northern analysis of miR-21 and miR-155 in KAI3 cells treated with both ASO-21 and ASO-155 and in cells treated with SCO-21 and SCO-155. (B) Western analysis of PTEN and SHIP1 and their downstream targets. Fold changes in protein levels are shown below the gels and are normalized to the level in SCO-treated cells, which was assigned a value of 1.00. (C) Incidence of apoptosis among KAI3 cells. Cells treated with both ASOs or SCOs were exposed to 50 μmol/L etoposide for 2 hours. (Top panels) Flow cytometric analysis is shown. y-axis: number of cells stained with PI; x-axis: cells stained with annexin V–FITC. Apoptotic cells are in R1 and R2; necrotic cells are in R3. (Bottom panel) □ and ■ indicate percentage of apoptosis (R1 + R2) or necrosis (R3) among SCO-21/155–treated and ASO-21/155–treated cells, respectively. Symbols and bars indicate means and SDs of triplicate samples. Both apoptotic (R1 + R2) and necrotic (R3) cells of ASO-21/155–treated cells show significantly greater percentages than those cells treated with SCO-21/155.

expression of pAKT in KAI3 cells. Moreover, the observation that MOTN1 cells transfected with miR-21 also showed enhanced activation of pAKT signaling suggests miR-21 and miR-155 also act together to enhance expression in the pAKT signaling pathway.

Our results demonstrate that overexpression of miR-21 and/or miR-155 play an essential role in NK-cell lymphomagenesis through activation of AKT signaling, which diminishes apoptosis (Bim down-regulation) and promotes cell-cycle progression (p21 and p27 down-regulation) and nuclear factorκB activation (phospho-p65 up-regulation). Among these, the proapoptotic protein Bim is the most likely the target of miR-21 during NK-cell lymphomagenesis because Bim disruption was repeatedly observed in our experiments. By contrast, miR-155 may control a variety of downstream targets via AKT disruption.

Discussion

Our data demonstrated that nearly all NK-cell lymphoma/leukemia lines, as well as specimens of primary lymphoma, overexpress miR-21, miR-155, or both. Interestingly, these 2 miRNAs were irreversibly expressed in both NK-cell lymphoma cell lines and patient samples. This finding suggests that miR-21 and miR-155, the functions of which are complementary, may contribute to lymphomagenesis through disruption of the same targets. Indeed, we found that these 2 miRNAs acted via PTEN and SHIP1, respectively, to regulate AKT, a serine-threonine kinase involved in various cellular functions, including the regulation of cell survival and proliferation. However, because our results were obtained from a limited numbers of samples, confirmation with the use of a larger number of test samples will be needed before we can conclude that the expression of these miRNAs in NK-cell lymphomas is actually irreversible. But irrespective of whether the expression patterns of these miRNAs are irreversible, the overexpression of either or both could play a key role in NK-cell lymphomagenesis.

miR-21 has been identified as the best hit in several medium-scale profiling experiments designed to detect miRNAs dysregulated in tumors, including cancers of the breast, colon, lung, pancreas, prostate, and stomach.[26] Recent studies indicate that miR-21 is also up-regulated in lymphomas/leukemias, including chronic lymphocytic leukemia, aggressive diffuse large B-cell lymphoma, both de novo and transformed cases, and follicular center lymphoma and Hodgkin lymphoma, whereas miR-155 is overexpressed in Burkitt lymphoma, chronic lymphocytic leukemia, and Hodgkin lymphoma.[27-32] However, there have been no studies investigating the involvement of miRNA in NK-cell lymphomas/leukemias; consequently, the roles played by miRNAs in the pathogenesis of these diseases remained largely unknown. In the present study, however, we found that miR-21 and miR-155 are both overexpressed in NK-cell lymphomas/leukemias. Furthermore, the expression levels of these miRNAs are significantly higher in NK-cell than in B-cell lymphomas/leukemias including EBV-positive B-cell lymphoma. How are these microRNAs overexpressed in NK-cell lymphomas?

In B-cell lymphoma, overexpression of miR-17-92 is caused by genomic amplification of the 13q31 locus.[8] miR-21 is located at 17q23, whereas miR-155 is at 21q21. Despite efforts by several groups[2-7] to detect specific genomic alterations in NK-cell lymphomas, no genomic amplifications or translocations of the 17q23 or 21q21 locus have been reported, which suggests genomic structural alterations are not involved in the up-regulation of these miRNAs in cancer.

One of possible alternative mechanism is infection of normal NK cells by EBV. Because nearly all NK-cell lymphomas/leukemias and endemic Burkitt lymphoma show infection by EBV, it is reasonable to suspect that the overexpression of these miRNAs is related to the virus. Consistent with that idea, recent reports suggest that EBV infection can lead directly to up-regulation of miR-21 and miR-155. For instance, Mrázek et al[33] reported that miR-21 is strongly up-regulated in EBV-infected human B lymphocytes, whereas Rahadiani et al[34] showed that EBV infection induces up-regulation of miR-155 in Burkitt lymphoma cell lines. Moreover, several groups[35-38] have shown that EBV-encoded LMP1 can induce transactivation of miR-155, which supports our idea that up-regulation of miR-21 and/or miR-155 by EBV infection is not limited to Burkitt lymphoma but also occurs in NK-cell lymphomas/leukemias. Up-regulation of these miRNAs via EBV infection could be the first-hit genetic alterations during NK-cell lymphomagenesis.

miRNAs are also up-regulated by oncogenic activation of transcription factors. For instance, expression of both miR-21 and miR-155 can be regulated by transcription factors such as AP-1.[39,40] Indeed, oncogenic transformation is frequently associated with enhancement of endogenous AP-1 activity mediated through various signal transduction pathways, which suggests AP-1–induced expression of miRNAs may also contribute to NK-cell lymphomagenesis.

In the present study, we found that miR-21 down-regulates the tumor suppressors PTEN and PDCD4. Meng et al[20] were the first to report that miR-21 regulates expression of PTEN and downstream PI3K signaling in human cholangiocarcinoma and hepatocellular carcinoma cells, and a corresponding modulation of PTEN protein expression by miR-21 was subsequently detected in a colon cancer cell line and during vascular neointimal lesion formation.[41,42] However, it remains unclear whether miR-21 regulates PTEN directly because the miR-21 binding site on the PTEN mRNA has not yet been characterized. Whether direct or not, regulation of PTEN by miR-21 appears to be cell type specific. miR-21 also down-regulated the tumor suppressor PDCD4, which is consistent with earlier findings that miR-21 directly down-regulates PDCD4 in breast, brain, and colorectal cancers.[43,44] PDCD4 inhibits PMA-induced neoplastic transformation, tumor promotion and progression, and intravasation,[45-47] which suggests its down-regulation by miR-21 could contribute to the aggressive clinicopathologic features of NK-cell lymphoma/leukemia, although we did investigate the mechanism by which PDCD4 functions in lymphomagenesis in the present study.

We found that miR-155 directly down-regulates SHIP1, which appears to regulate both p21 and p27 via pAKT in MOTN1 cells, suggesting SHIP1 can affect cell-cycle progression via the AKT-signaling pathway. Horn et al[48] showed that forced expression of SHIP1 in Jurkat cells, a T-cell leukemia cell line, induces G_1-S arrest by repressing p27, and Freeburn et al[49] showed that SHIP1 can influence the constitutive levels of PI(3,4,5)P(3) and the activity of downstream PI3K effectors, including AKT, in T lymphocytes. These results strongly support our finding that SHIP1 down-regulates p21 and p27 via the AKT pathway. Moreover, it was very recently reported that endogenous expression of SHIP1 is repressed in hematopoietic cells overexpressing miR-155 in vitro and in vivo, which leads to increased activation of AKT.[50] This, too, is consistent with our findings.

In summary, we have shown that dysregulation of miRNAs is a key feature of the pathogenesis of NK-cell lymphoma/leukemia. Overexpression of miR-21 and/or miR-155, which might be up-regulated by EBV infection, affects AKT signaling via their respective repression of PTEN and SHIP1. These findings provide new insight into the pathogenesis of NK-cell lymphoma/leukemia and suggest targeting miR-21 and/or miR-155 may represent a useful approach to treating NK-cell lymphoma/leukemia.

Acknowledgments

We wish to express our appreciation to A. Kobayashi, B. Kataho, and C. Kikuchi (Akita University) for their outstanding technical assistance; and Drs M. Saitoh, M. Kume, and S. Takahashi (Hiraka General Hospital) and H. Nanjo (Akita University) for histologic and/or clinical diagnosis of lymphoma. pMX vector was kindly provided by Dr T. Kitamura (Tokyo University).

This work was supported in by the Grant-in-Aid Scientific Research (C) from the Japan Society for the Promotion of Science (to H.T.) and by the Grant Global Center of Excellence Program (G-COE) of the Ministry of Education, Science, Technology, Sports, and Culture of Japan (to K.S.).

Authorship

Contribution: Y.Y. performed experiments, analyzed data, and constructed the tables; A.W.,Y.-M. G., K.I., and J.Y. performed the experiments; N.T., H.S., Y.K., N.S., R.I., N.T., and K.S. analyzed data; and H.T. designed and performed experiments, analyzed data, wrote the paper, and organized the study.

Conflict-of-interest disclosure: The authors declare no competing financial interests.

Correspondence: Hiroyuki Tagawa, MD, PhD, Department of Hematology, Nephrology, and Rheumatology, Akita University Graduate School of Medicine, 1-1-1 Hondo, Akita 0108543, Japan; e-mail: htagawa0279jp@yahoo.co.jp.

References

1. Jaffe ES, Harris NL, Stein H, Campo E, Pileri SA, Swerdlow SH. Introduction and over review of the classification of the lymphoid neoplasms. In: Swerdloe AH, Campo E, Harris NL, et al, eds. *World Health Classification of Tumors: Pathology & Genetics of Tumors of Haematopoietic and Lymphoid Tissues*. Lyon: IARC Press; 2008:158-178.
2. Siu LL, Wong KF, Chan JFC, Kwong YL. Comparative genomic hybridization analysis of natural killer cell lymphoma. *Am J Pathol*. 1999;155(5):1419-1425.
3. Siu LL, Chan V, Chan JKC, Wong KF, Liang R, Kwong YL. Consistent patterns of allelic loss in natural killer cell lymphoma. *Am J Pathol*. 2000; 157(6):1803-1809.
4. Wong KF, Zhang YM, Chan KFC. Cytogenetic abnormalities in natural killer cell lymphoma/leukemia—is there a consistent pattern? *Leuk Lymphoma*. 34(3-4):241-250, 1999.
5. Yoon J, Ko YH. Deletion mapping of the long arm of chromosome 6 in peripheral T and NK cell lymphomas. *Leuk Lymphoma*. 2003;44(12):2077-2082.
6. Ko YH, Choi KE, Han JH, Kim JM, Ree HJ. Comparative genomic hybridization study of nasal-type NK/T-cell lymphoma. *Cytometry*. 2001;46(2): 85-91.
7. Nakashima Y, Tagawa H, Suzuki R, et al. Genome-wide array-based comparative genomic hybridization of natural killer cell lymphoma/leukemia: different genomic alteration patterns of

aggressive NK-cell leukemia and extranodal NK/T lymphoma, nasal type. *Genes Chromosomes Cancer.* 2005;19(3):247-255.

8. Inomata M, Tagawa H, Guo Y-M, Kameoka Y, Takahashi N, Sawada K. MicroRNA-17-92 downregulates expression of distinct targets in different B-cell lymphoma subtypes. *Blood.* 2009;113(2): 396-402.
9. Robertson MJ, Cochran KJ, Cameron C, Le J-M, Tantravahi R, Ritz J. Characterization of a cell line, NKL, derived from an aggressive human natural killer cell leukemia. *Exp Hematol.* 1996; 24(3):406-415.
10. Yagita M, Huang CL, Umehara H, et al. A novel natural killer cell line (KHYG1) from a patient with aggressive natural killer cell leukemia carrying p53 point mutation. *Leukemia.* 2000;14(5):922-930.
11. Yodoi J, Teshigawara K, Nikaido T, et al. TCGF(IL2)-receptor inducing factor(s). I. Regulation of IL2 receptor on a natural killer-like cell line (YT cells). *J Immunol.* 1985;134(3):1623-1630.
12. Tsuge I, Morishima T, Morita M, Kimura H, Kuzushima K, Matsuoka H. Characterization of Epstein-Barr virus (EBV)-infected natural killer (NK) cell proliferation in patients with severe mosquito allergy; establishment of an IL-2-dependent NK-like cell line. *Clin Exp Immunol.* 1999;115(3): 385-392.
13. Gong JH, Maki G, Kingemann HG. Characterization of a human cell line (NK-92) with phenotypical and functional characteristics of active natural killer cells. *Leukemia.* 1994;8(4):652-658.
14. Kagami Y, Nakamura S, Suzuki R, et al. Establishment of an IL-2-dependent cell line derived from 'nasal-type' NK/T-cell lymphoma of $CD2^+$,$sCD3^-$,$CD3e^+$,$CD56^+$ phenotype and associated with the Epstein-Barr virus. *Br J Haematol.* 1998;103(3):669-677.
15. Kanno H, Watabe D, Shimizu N, Sawai T. Adhesion of Epstein-Barr virus-positive natural killer cell lines to cultured endothelial cells stimulated with inflammatory cytokines. *Clin Exp Hematol.* 2008;151(3):519-527.
16. Nagata H, Konno A, Kimura N, et al. Characterization of novel natural killer (NK)-cell and gamma delta T cell lines established from primary lesions of nasal T/NK cell lymphomas associated with Epstein-Barr virus. *Blood.* 2001;97(3):708-713.
17. Di Noto RD, Pane F, Camera A, et al. Characterization of two novel cell lines, DERL-2 ($CD56^+$/$CD3^+$/TCR gamma $\gamma\delta^+$) and DERL-7 ($CD56^+$/$CD3^-$/TCR $\gamma\delta$-), derived from a single patient with $CD56^+$ non Hodgkin's lymphoma. *Leukemia.* 2001;15(10):1641-1649.
18. Matsuo Y, Drexler HG, Takeuchi M, Tanaka M, Orita K. Establishment of the T-cell large granular lymphocyte leukemia cell line MOTN-1 caring natural killer-cell antigens. *Leuk Res.* 2002;26(9): 873-879.
19. Frankel LB, Christoffersen NR, Jacobsen A, Lindow M, Krogh A, Lund AH. Programmed cell death 4(PDCD4) is an important functional target of the microRNA-21 in breast cancer cells. *J Biol Chem.* 2008;283(2):1026-1033.
20. Meng F, Henson R, Wehbe-Janek H, Ghoshal K, Jacob ST, Patel T. MicroRNA-21 regulates expression of Pten tumor suppressor gene in Human hepatocellular cancer. *Gastroenterology.* 2007;133(2):647-658.
21. Lewis BP, Shih IH, Jones-Rhoades MW, Bartel DP, Burge CB. Prediction of mammalian microRNA targets. *Cell.* 2003;115(7):787-798.
22. Thum T, Gross C, Fiedler J, et al. MicroRNA-21 contributes to myocardial disease by stimulating MAP kinase signaling in fibroblasts. *Nature.* 2008;456(7224):980-984.
23. Sayed D, Rane S, Lypowy J, et al. MicroRNA-21 targets Sprouty2 and promotes cellular outgrowths. *Mol Biol Cell.* 2008;19(8):3272-3282.
24. O'Connor L, Strasser A, O'Reilly LA, et al. Bim: a novel member of the Bcl-2 family that promotes apoptosis. *EMBO J.* 1998;17(2):384-395.
25. Stahl M, Dijkers PF, Kops GJ, et al. The forkhead transcription factor FoxO regulates transcription of p27Kip1 and Bim in response to IL-2. *J Immunol.* 2002;168(10):5024-5031.
26. Volinia S, Calin GA, Liu CG, et al. A microRNA expression signature of human solid tumors defines cancer gene targets. *Proc Natl Acad Sci U S A.* 2006;103(7):18225-18260.
27. Fulci V, Chiaretti S, Goldoni M, et al. Quantitative technologies establish a novel microRNA profile of chronic lymphocytic leukemia. *Blood.* 2007; 109(11):4944-4951.
28. Lawrie CH, Soneji S, Marafioti T, et al. MicroRNA expression distinguishes between germinal center B cell-like and activated B cell-like subtypes of diffuse large B-cell lymphoma. *Int J Cancer.* 2007;121(5):1156-1161.
29. Navarro A, Gaya A, Martinez A, et al. MicroRNA expression profiling in classic Hodgkin lymphoma. *Blood.* 2008;111(5):2825-2832.
30. Kluiver J, Poppema S, de Jong D, et al. BIC and miR-155 are highly expressed in Hodgkin, primary mediastinal and diffuse large B cell lymphomas. *J Pathol.* 2005;207(2):243-249.
31. Kluiver J, van den Berg A, de Jong D, et al. Regulation of pri-microRNA BIC transcription and processing in Burkitt lymphoma. *Oncogene.* 2007; 26(26):3769-3776.
32. Marton S, Garcia MR, Robello C, et al. Small RNAs analysis in CLL reveals a deregulation of miRNA expression and novel miRNA candidates of putative relevance in CLL pathogenesis. *Leukemia.* 2008;22(2):330-338.
33. Mrázek J, Kreutmayer SB, Friedrich A. Grässer FA, Polacek N, Huttenhofer A. Subtractive hybridization identifies novel differentially expressed ncRNA species in EBV-infected human B cells. *Nucleic Acids Res.* 2007;35(10):e73.
34. Rahadiani N, Takakuwa T, Tresnasari K, Morii E, Aozasa K. Latent membrane protein-1 of Epstein-Barr virus induces the expression of B-cell integration cluster, a precursor form of microRNA-155, in B lymphoma cell lines. *Biochem Biophys Res Commun.* 2008;377(2):579-583.
35. Motsch N, Pfuhl T, Mrazek J, Barth S, Grässer FA. Epstein-Barr virus-encoded latent membrane protein 1 (LMP1) induces the expression of the cellular microRNA miR-146a. *RNA Biol.* 2007; 4(3):131-137.
36. Yin Q, McBride J, Fewell C, et al. MicroRNA-155 is an Epstein-Barr virus-induced gene that modulates Epstein-Barr virus-regulated gene expression pathways. *J Virol.* 2008;82(11):5295-5306.
37. Lu F, Weidmer A, Liu CG, Volinia S, Croce CM, Lieberman PM. Epstein-Barr virus-induced mir-155 attenuates NK-κB signaling and stabilizes latent virus persistence. *J Virol.* 2008;82(21): 10436-10443.
38. Gatto G, Rossi A, Rossi D, Kroeninig S, Bonatti S, Mallardo M. Epstein-Barr virus latent membrane protein 1 trans-activates miR-155 transcription through the NF-kB pathway. *Nucleic Acids Res.* 2008;36(20):6608-6619.
39. Fujita S, Ito T, Mizutani T, et al. miR-21 gene expression triggered by AP-1 is sustained through a double-negative feedback mechanism. *J Mol Biol.* 2008;378(3):492-504.
40. Yin Q, Wang X, McBride J, Fewell C, Flemington E. B-cell receptor activation induce BIC/miR-155 expression through a conserved AP-1 element. *J Biol Chem.* 2008;283(5):2654-2662.
41. Asangani IA, Rasheed SA, Nikolova DA, et al. MicroRNA-21 (miR-21) post-transcriptionally downregulates tumor suppressor Pdcd4 and stimulates invasion, intravasation and metastasis in colorectal cancer. *Oncogene.* 2008;27(15): 2128-2136.
42. Ji R, Cheng Y, Yue J, et al. MicroRNA expression signature and antisense-mediated depletion reveal an essential role of microRNA in vascular neointimal lesion formation. *Circ Res.* 2007; 100(11):1579-1588.
43. Frankel LB, Christoffersen NR, Jacobsen A, Lindow M, Krogh A, Lund AH. Programmed cell death 4 (PDCD4) is an important functional target of the microRNA miR-21 in breast cancer cells. *J Biol Chem.* 2008;283(2):1026-1033.
44. Gabriely G, Wurdinger T, Kesari S, et al. MicroRNA 21 promotes glioma invasion by targeting matrix metalloproteinase regulators. *Mol Cell Biol.* 2008;28(17):5369-5380.
45. Cmarik JL, Min H, Hegamyer G, et al. Differentially expressed protein Pdcd4 inhibits tumor promoter-induced neoplastic transformation. *Proc Natl Acad Sci U S A.* 1999;96(24):14037-14042.
46. Jansen AP, Camalier CE, Colburn NH. Epidermal expression of the translation inhibitor programmed cell death 4 suppresses tumorigenesis. *Cancer Res.* 2005;65(14):6034-6041.
47. Leupold JH, Yang HS, Colburn NH, Asangani I, Post S, Allgayer H. Tumor suppressor Pdcd4 inhibits invasion/intravasation and regulates urokinase receptor (u-PAR) gene expression via Sp-transcription factors. *Oncogene.* 2007;26(31): 4550-4562.
48. Horn S, Endl E, Fehse B, Weck MM, Mayr GW, Jucker M. Restoration of SHIP activity in a human leukemia cell line downregulates constitutively activated phosphatidylinositol 3-kinase/Akt/GSK-3b signaling and leads to an increased transit time through the G1 phase of the cell cycle. *Leukemia.* 2004;18(11):1839-1849.
49. Freeburn RW, Wright K, Burgess SJ, Astoul E, Cantrell DA, Ward SG. Evidence that SHIP-1 contributes to phosphatidilinositol 3,4,5-trisphosphate metabolism in T lymphocytes and can regulate novel phosphoinositide 3-kinase effectors. *J Immunol.* 2002;169(10):5441-5450.
50. O'Connell RM, Chaudhuri AA, Rao DS, Baltimore D. Inositol phosphatase SHIP1 is a primary target of miR-155. *Proc Natl Acad Sci U S A.* 2009; 106(17):7113-7118.

Journal of Pathology
J Pathol 2010; **221**: 164–174
Published online 18 February 2010 in Wiley InterScience
(www.interscience.wiley.com) DOI: 10.1002/path.2699

ORIGINAL PAPER

Interleukin-2 induces NF-κB activation through BCL10 and affects its subcellular localization in natural killer lymphoma cells

Ka-Kui Chan,[1] Lijun Shen,[1] Wing-Yan Au,[2] Hiu-Fung Yuen,[1] Kai-Yau Wong,[1] Tianhuan Guo,[1] Michelle LY Wong,[1] Norio Shimizu,[3] Junjiro Tsuchiyama,[4] Yok-Lam Kwong,[2] Raymond HS Liang[2] and Gopesh Srivastava[1]*

[1] *Department of Pathology, The University of Hong Kong, Queen Mary Hospital, Hong Kong, China*
[2] *Department of Medicine, The University of Hong Kong, Queen Mary Hospital, Hong Kong, China*
[3] *Medical Research Institute, Tokyo Medical and Dental University, Tokyo, Japan*
[4] *Department of Pathology, Kawasaki Medical School, Kurashiki, Okayama, Japan*

**Correspondence to: Gopesh Srivastava, Lymphoma Research Laboratory, Department of Pathology, The University of Hong Kong, Queen Mary Hospital, Pokfulam, Hong Kong, China. e-mail: gopesh@pathology.hku.hk*

Abstract

Deregulation of nuclear factor (NF)-κB signalling is common in cancers and is essential for tumourigenesis. Constitutive NF-κB activation in extranodal natural killer (NK)-cell lymphoma, nasal type (ENKL) is known to be associated with aberrant nuclear translocation of BCL10. Here we investigated the mechanisms leading to NF-κB activation and BCL10 nuclear localization in ENKLs. Given that ENKLs are dependent on T-cell-derived interleukin-2 (IL2) for cytotoxicity and proliferation, we investigated whether IL2 modulates NF-κB activation and BCL10 subcellular localization in ENKLs. In the present study, IL2-activated NK lymphoma cells were found to induce NF-κB activation via the PI3K/Akt pathway, leading to an increase in the entry of G_2/M phase and concomitant transcription of NF-κB-responsive genes. We also found that BCL10, a key mediator of NF-κB signalling, participates in the cytokine receptor-induced activation of NF-κB. Knockdown of BCL10 expression resulted in deficient NF-κB signalling, whereas Akt activation was unaffected. Our results suggest that BCL10 plays a role downstream of Akt in the IL2-triggered NF-κB signalling pathway. Moreover, the addition of IL2 to NK cells led to aberrant nuclear translocation of BCL10, which is a pathological feature of ENKLs. We further show that BCL10 can bind to BCL3, a transcriptional co-activator and nuclear protein. Up-regulation of BCL3 expression was observed in response to IL2. Similar to BCL10, the expression and nuclear translocation of BCL3 were induced by IL2 in an Akt-dependent manner. The nuclear translocation of BCL10 was also dependent on BCL3 because silencing BCL3 by RNA interference abrogated this translocation. We identified a critical role for BCL10 in the cytokine receptor-induced NF-κB signalling pathway, which is essential for NK cell activation. We also revealed the underlying mechanism that controls BCL10 nuclear translocation in NK cells. Our findings provide insight into a molecular network within the NF-κB signalling pathway that promotes the pathogenesis of NK cell lymphomas. Copyright © 2010 Pathological Society of Great Britain and Ireland. Published by John Wiley & Sons, Ltd.

Keywords: NK cell lymphoma; IL2; nucleus; BCL10; NF-κB

Received 21 August 2009; Revised 4 January 2010; Accepted 3 February 2010

No conflicts of interest were declared.

Introduction

Extranodal natural killer (NK)-cell lymphoma, nasal type (ENKL) is a major NK cell malignancy that occurs in Asia and Central and South America. Most cases are of NK cell origin, exhibiting CD56 but lacking surface CD3 expression [1]. Immunohistochemistry shows that the tumour cells display an activated NK cell phenotype, with the expression of various cytolytic lymphocyte-associated proteins and surface markers [2,3]. Previously, we reported that constitutive nuclear factor (NF)-κB activation is present in ENKLs but not in resting normal NK cells [4]. This phenotype was also strongly associated with another specific molecular feature, the nuclear translocation of BCL10 in ENKL cells ($p = 0.001$). The underlying molecular mechanisms of this disease, however, are still elusive.

The *BCL10* gene was originally identified from the recurrent involvement of t(1;14)(p22;q32) in gastric mucosa-associated lymphoid tissue (MALT) lymphoma and encodes a cytosolic protein composed of 233 amino acids with pro-inflammatory activity [5]. Nuclear translocation of BCL10 occurs frequently in MALT lymphomas with t(1;14)(p22;q32) and t(11;18)(q21;q21) [6], resulting in more BCL10 protein in tumour cells via the overexpression or stabilization of the protein [7,8]. ENKLs do not harbour these chromosomal aberrations; thus, it is not likely that the same mechanism accounts for the presence of nuclear BCL10 in ENKLs. An alternative mechanism responsible for the same feature of nuclear translocation of BCL10 in ENKLs must exist.

BCL10 is a molecular adaptor that mediates canonical NF-κB signalling in T and B lymphocytes [9–11]. It forms a signalosome along with CARMA1 and MALT1 to relay the antigen receptor signals that activate IKKγ [12]. When the IKK complex is activated, the NF-κB inhibitor IκBα is degraded and NF-κB is allowed to enter the nucleus to induce the transcription of numerous NF-κB-responsive genes. Recent studies have shown that rather than cytotoxicity, the selective role of BCL10 mediates cytokine production when ITAM-coupled NK cell receptors are engaged [13,14]. In contrast to the well-characterized antigen receptor-induced NF-κB signalling, the role of BCL10 in cytokine receptor signalling remains elusive.

Cytokine deregulation is closely associated with the pathogenesis of haematological diseases and cytokine expression patterns sometimes have diagnostic value [15,16]. Notably, interleukin-2 (IL2) is a potent cytokine that promotes the proliferation of primary NK cells. In addition, most of the NK cell lines derived from ENKL are IL2-dependent [17–19]. It is conceivable that IL2 is a survival factor for tumour cells. Moreover, IL2 can cause NF-κB activation; however, the link between the IL2 receptor and NF-κB is less clearly defined [20]. The signalling pathways triggered by the IL2 receptor are diverse and include the JAK/STAT, PI3K/Akt, and Ras/MAPK pathways [21,22]. Among these, Akt was shown to regulate the induction of NF-κB in Jurkat cells and act as a stimulatory signal triggered by antigen engagement, which involves BCL10 [23,24]. We examined the role of Akt and BCL10 in ENKL cells in the cytokine receptor-triggered signalling cascades. Tumour necrosis factor-α (TNF-α), another cytokine, has been shown to induce BCL10 nuclear localization in breast cancer cells [25], suggesting that cytokine stimulation may be one of the contributing factors to aberrant nuclear BCL10 expression. We investigated the effect of IL2 stimulation on BCL10 subcellular localization in NK lymphoma cells to demonstrate the underlying molecular mechanisms.

Materials and methods

Cell lines and reagents

The human NK cell lines SNK-6 and NK-YS of ENKL origin [26] were maintained in RPMI 1640 medium (Hyclone, Logan, UT, USA) supplemented with 10% fetal bovine serum, 2 mM L-glutamine, 100 U/ml penicillin, and 100 μg/ml streptomycin. The cells were routinely cultured with a supplement of 100 U/ml recombinant human IL2 (PeproTech, London, UK). Before the experiments, both cell lines were starved of IL2 for 48 h and then treated with IL2 for 4 h, unless otherwise specified. Cycloheximide (CHX) and Akt inhibitor I (Akt-I) (Calbiochem, Merck Biosciences, Darmstadt, Germany) were dissolved in ethanol and dimethyl sulphoxide (DMSO), respectively, and added 30 min before the addition of IL2 in some experiments. The antibodies used in the study are described in the Supporting information, Supplementary Table 1.

Isolation of normal NK cells

Normal NK cells were isolated from the peripheral blood of two healthy volunteers using the Dynal® NK Cell Negative Isolation Kit (Dynal Biotech, Oslo, Norway). The purity of the NK cells was verified by flow cytometry and found to be over 95%. The normal NK cells were cultured under the same conditions as those described above for the NK cell lines.

RT-PCR analysis

Total RNA was extracted using TRIzol reagent (Invitrogen, Carlsbad, CA, USA). The first-strand cDNA was synthesized from 2 μg of RNA using oligo $d(T)_{16}$ and the GeneAmp RNA PCR Kit (Applied Biosystems, Foster City, CA, USA). Semi-quantitative RT-PCR was performed to detect granzyme B, perforin, *BCL3*, and *GAPDH* mRNA transcripts using AmpliTaq Gold polymerase (Applied Biosystems). The primers used are described in the Supporting information, Supplementary Table 2. The sequences of the primers used for quantitative RT-PCR for granzyme B, perforin, and actin mRNA transcripts are described in the Supporting information, Supplementary Table 3. Products were stained with SYBR Green (Molecular Probes, Eugene, OR, USA) and analysed using a 7700 Real-Time PCR System (Applied Biosystems).

Yeast two-hybrid screening

Yeast two-hybrid screening was performed using the Matchmaker Two-Hybrid System 3 (Clontech, Mountain View, CA, USA). The cDNA library was generated from the RNA of SNK-6 cells. Small-scale library transformation and screening were performed, and potential positive colonies were analysed by PCR screening and sequencing. Putative interactions were further confirmed by co-immunoprecipitation from the cell lines.

Co-immunoprecipitation and western blotting

Cells were lysed in RIPA buffer (Santa Cruz Biotechnology, Santa Cruz, CA, USA). Protein concentrations were measured using the Bio-Rad DC Protein Assay Kit (Bio-Rad, Hercules, CA, USA). Proteins were immunoprecipitated with antibodies or isotype-matched immunoglobulin at 4 °C overnight. The bound protein–antibody complexes were pulled down with protein G plus-agarose (Santa Cruz Biotechnology). The products were resolved by 10% SDS-PAGE and transferred to a PVDF membrane. The membrane was blocked with 5% non-fat milk and incubated with the primary antibody at 4 °C overnight or at room temperature for 1 h. After washing with TBST, the membrane was incubated with an HRP-conjugated secondary antibody for 1 h at room temperature. Signals were detected using Hyperfilm with ECL plus reagent (Amersham Biosciences, Piscataway, NJ, USA).

Cellular fractionation

Cells were lysed with 10 mM HEPES containing 1.5 mM $MgCl_2$, 10 mM KCl, 0.5 mM DTT, 0.5 mM PMSF, and 0.2% Nonidet P-40 supplemented with a cocktail of protease inhibitors. Lysates were placed on ice for 10 min and separated by centrifugation at 3000 rpm for 10 min. The supernatant was collected as the cytoplasmic fraction and the cell pellet was further lysed with buffer containing 50 mM Tris (pH 8.0), 500 mM NaCl, 5 mM EDTA, 0.5 mM DTT, 0.5 mM PMSF, 1% Nonidet P-40, and protease inhibitors at 4 °C for 30 min. The supernatant was collected as the nuclear fraction following centrifugation at 13 000 rpm for 10 min at 4 °C.

Electromobility shift assay (EMSA)

The NF-κB oligonucleotide consensus probe and gel shift assay system were purchased from Promega (Madison, WI, USA). The oligonucleotide was labelled with [γ-^{32}P]ATP using a T4 polynucleotide kinase and the unincorporated radionucleotides were removed using MicroSpin G25 columns. Cells were harvested and nuclear protein fractions were collected. Equal amounts of nuclear extracts were incubated with the radioactive probe according to the user manual. For the supershift assay, antibodies against p50 or p65 were added to the reaction mixture and incubated at 4 °C for 1 h. The DNA–protein complexes were resolved in a 5% polyacrylamide gel. The gel was then dried and exposed to X-ray film at −70 °C.

RNA interference with shRNA

Complementary oligonucleotides (Supporting information, Supplementary Table 4) were annealed and ligated with the pSIREN-RetroQ vector using the knockout RNAi system (Clontech). A negative control shRNA oligonucleotide against luciferase (shCon) was provided by the RNAi system. Transfection of the packaging cell line, PT67, was performed using FuGene 6 transfection reagent (Roche, Mannheim, Germany). The medium containing the viral particles was collected 2 days after transfection. The supernatant was filtered through a 0.45 μm filter and polybrene (8 μg/ml) (Sigma-Aldrich, St. Louis, MO, USA) was then added. SNK-6 cells were incubated with the virus-containing supernatant for 24 h and the supernatant was replaced with fresh RPMI medium. Infected cells were collected 1 day later.

Flow cytometry

Cells were collected by centrifugation and washed twice with PBS. The cell pellets were fixed overnight with ice-cold 70% ethanol and the cells were then resuspended in PBS containing 200 μg/ml RNase A and 20 μg/ml propidium iodide (Sigma-Aldrich). The samples were examined using a FACS Calibur flow cytometer (BD Bioscience, San Jose, CA, USA) and the Cell Quest program. Proportions of cells in different phases were quantified with ModFit LT software (Verity Software House, Topsham, ME, USA).

Immunofluorescence microscopy

Cells were collected and cytospun onto slides. After fixation with cold methanol, the slides were incubated with the primary antibody at 4 °C overnight. After washing, a fluorescein isothiocyanate (FITC)-conjugated secondary antibody (Chemicon, Temecula, CA, USA) was applied to the slides. Cell nuclei were counterstained with 4′,6-diamidino-2-phenylindole (DAPI; Roche) and signals were visualized using an Eclipse E800M microscope (Nikon, Tokyo, Japan).

Statistics

The data were compared using the t-test and $p < 0.05$ was regarded to be statistically significant.

Results

IL2 induces NF-κB activation via Akt

To determine whether PI3K and Akt were engaged in IL2-induced NF-κB signalling, two bona fide ENKL cell lines, SNK-6 and NK-YS [26], were treated with IL2 prior to analysis. IL2 stimulation resulted in the binding of NF-κB to its consensus sequences, as shown by the EMSA (Figure 1a), which demonstrated that IL2 activates NK tumour cells via the canonical NF-κB pathway involving the p65/p50 heterodimer. Consistently, more of the p65 subunit was detected in nuclear extracts from ENKL cells grown in the presence of IL2, while its cytosolic counterpart was unchanged (Figure 1b).

To address the role of Akt in this process, we treated the cells with an Akt-specific inhibitor (Akt-I) [27] before the addition of IL2. Akt-I is a phosphatidylinositol ether analogue that binds to the pleckstrin homology domain of Akt. We used a dosage of Akt-I that does not affect cell viability or PI3K ($IC_{50} = 83$ μM), such that other PI3K-related downstream signalling molecules remained unaffected. The addition of Akt-I inhibited the nuclear translocation of p65 and the binding of NF-κB to its consensus sequences (Figures 1a and 1b). To demonstrate the specific effect of this inhibitor on Akt activity, we examined the phosphorylation status of the Ser^{473} residue, a hallmark of Akt activation. As expected, Akt phosphorylation was increased in the cells treated with IL2 alone, whereas treatment of the cells with Akt-I for 4 h suppressed IL2-induced Akt phosphorylation (Figure 1c).

To evaluate NF-κB activity further under these conditions, semi-quantitative RT-PCR was performed to examine the RNA transcript levels of granzyme B and perforin. Granzyme B and perforin are the two major components of NK cell cytolytic granules and their genes are responsive to NF-κB [20,28]. The RT-PCR results showed that IL2 enhances the transcription

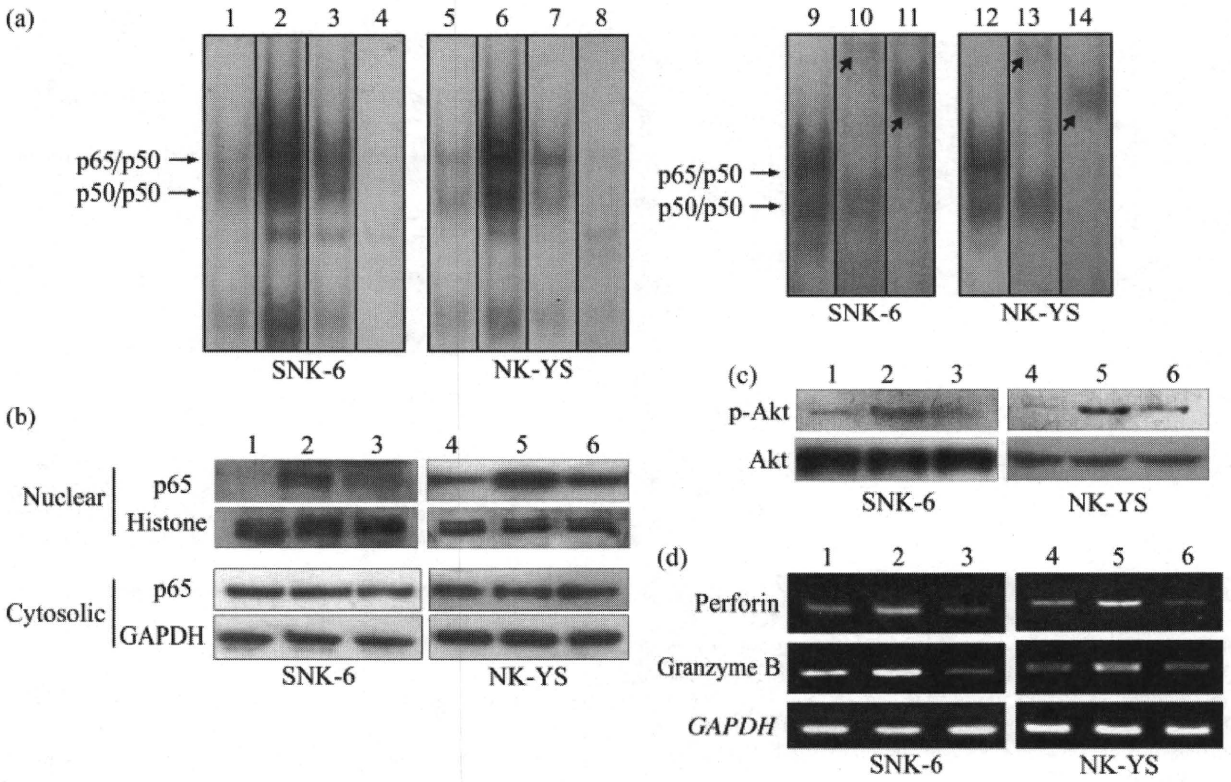

Figure 1. Activation of NF-κB via Akt. (a) EMSA results of NK cell lines SNK-6 and NK-YS. Cells were deprived of IL2 (1 and 5) or treated with 300 U/ml of IL2 alone (2, 6, 9, and 12) or IL2 together with 10 μM Akt-I (3 and 7). In the supershift assay, nuclear lysates were incubated with either p65 antibody (10 and 13) or p50 antibody (11 and 14) to identify the position (short-tailed arrows) of the p65/p50 heterodimer and the p50 homodimer. A cold competitor of the NF-κB consensus sequence was added as a control (4 and 8). (b) Immunoblotting results for p65 in nuclear and cytosolic extracts from the SNK-6 and NK-YS cell lines. GAPDH was used for the normalization of cytosolic proteins and histone H1 was used for the normalization of nuclear proteins. (c) Immunoblotting results for phospho-Akt (Ser^{473}), with total Akt used as the normalization control. (d) Semi-quantitative RT-PCR results for perforin and granzyme B. *GAPDH* was used for normalization. For b, c, and d, cells were deprived of IL2 (1 and 4) or treated with 300 U/ml IL2 alone (lanes 2 and 5) or IL2 together with 10 μM Akt-I (lanes 3 and 6).

of granzyme B and perforin, whereas Akt-I blocked this effect (Figure 1d).

IL2-induced NF-κB activation is BCL10-dependent

To explore the potential role of BCL10 in cytokine receptor signalling, the expression of BCL10 was knocked down using an shRNA specifically targeting BCL10. As demonstrated by western blot, sequence B suppressed BCL10 expression more effectively than sequence A (Figure 2a). Depletion of BCL10 rendered the SNK-6 cells less responsive to IL2 with regard to NF-κB activation, compared with treatment with the control sequence (Figure 2b). To rule out off-target silencing effects on Akt activation due to the shRNA, we again measured the levels of Akt phosphorylation in cells treated with shRNA. As shown in Figure 2c, no remarkable changes in Akt phosphorylation levels were observed between the mock control and the shRNA-treated cells. These results suggest that BCL10 participates in IL2-mediated NF-κB signalling and likely plays a role downstream of Akt.

We then examined the transcription of the cytolytic genes perforin and granzyme B, which is responsive to NF-κB. As expected, depletion of BCL10 resulted

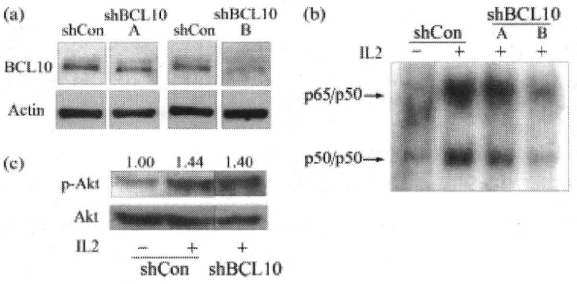

Figure 2. Knockdown of BCL10 expression inhibits IL2-induced NF-κB activation. (a) Immunoblotting results for BCL10 in SNK-6 cells. BCL10 expression was knocked down using two shRNA sequences (shBCL10-A and -B). A luciferase sequence (shCon) was used as a negative control. Actin served as the normalization control for immunoblotting. (b) EMSA results showing the changes in NF-κB activity in SNK-6 cells. (c) Immunoblotting results for phospho-Akt (p-Akt) in SNK-6 cells, with total Akt used as a normalization control. Band density was measured with Grab-IT (Ultra Violet Products Ltd, Cambridge, UK). The p-Akt to Akt ratio is shown at the top of the panel for comparison.

in a decline in the transcription of both perforin and granzyme B (Figure 3a). Furthermore, alterations in NF-κB activity were demonstrated by cell cycle analysis because the up-regulation of NF-κB activity

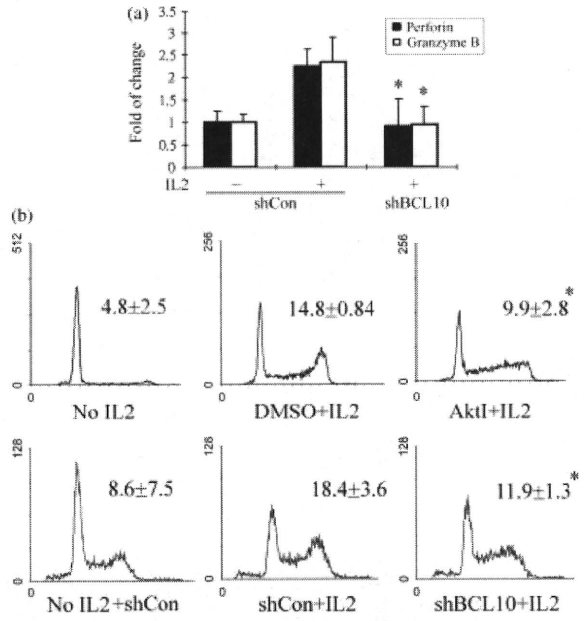

Figure 3. Knockdown of BCL10 suppresses IL2-induced gene transcription and restricts the number of cells in the G_2/M phase. (a) Quantitative RT-PCR results for perforin and granzyme B in SNK-6 cells. shRNA-transduced cells were treated in the presence or absence of IL2 as specified in the figure. (b) Blocking Akt or silencing BCL10 with shRNA reduced the percentage of SNK-6 cells in the G_2/M phase. DMSO was the vehicle control for Akt-I. A luciferase sequence (shCon) was used as a negative control for RNA interference in a and b. Each histogram is representative of three independent experiments. The percentage of cells in the G_2/M phase from three experiments is shown as the mean ± SD (*$p < 0.05$ when compared with the corresponding negative or vehicle control).

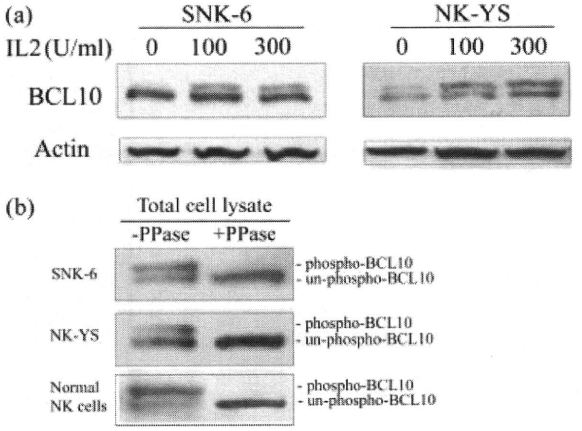

Figure 4. IL2 induces an increase in the total and phosphorylated forms of BCL10. (a) Immunoblotting results for BCL10 in NK cell lines treated with different concentrations of IL2. β-Actin served as the loading control. (b) Identification of phospho-BCL10 by phosphatase (λ-PPase) treatment and immunoblotting. Total cell lysates were incubated in the presence or absence of phosphatase for 4 h before western blotting.

usually allows more cells to undergo cell division [29]. The addition of IL2 induced more SNK-6 cells to enter the cell cycle, with an increase in the percentage of cells in the G_2/M phase, but this effect could be suppressed by either Akt-I or shBCL10-B (Figure 3b).

IL2 promotes the overexpression and phosphorylation of BCL10

The *BCL10* gene has been suggested to be responsive to NF-κB [25]; we therefore examined the expression level of BCL10 in both cell lines treated with different concentrations of IL2. Incubation with IL2 for 4 h could either increase the total expression level or promote the phosphorylation of BCL10, but the results were slightly different between the two cell lines (Figure 4). In SNK-6 cells, there was an increase in the phosphorylated form of BCL10, but changes in the unphosphorylated form were not evident. In NK-YS cells, both forms seemed to be increased simultaneously along with IL2 in a dose-dependent manner.

IL2 induces BCL10 translocation to the nucleus

In addition to up-regulation of BCL10, IL2 stimulation could trigger the nuclear translocation of BCL10 in NK cells. The malignant cell lines (SNK-6 and NK-YS) and normal NK cells were cultured without the addition of IL2 for 2 days before they were stimulated with IL2. The addition of IL2 resulted in more BCL10 in the nucleus compared with the IL2-deprived cells. This phenomenon was observed not only in both ENKL cell lines, but also in IL2-activated NK cells from healthy individuals; thus, it was a result of the activation of NK cells rather than a lymphoma-specific effect. The BCL10 in the nucleus formed large granules with irregular shapes (Figure 5a). Moreover, the western blot results were consistent with the finding that BCL10 levels increased significantly in nuclear extracts upon IL2 stimulation (Figure 5b), while they increased only slightly in the cytosolic extracts. Like its cytosolic counterpart, nuclear BCL10 was also made up of both phosphorylated and unphosphorylated forms, suggesting that BCL10 phosphorylation alone is not sufficient for nuclear translocation. The nuclear translocation was Akt-dependent, however, as the addition of Akt-I reduced the amount of nuclear BCL10 but did not change that of cytosolic BCL10 (Figure 5c).

BCL3 is a binding partner of BCL10

The translocation of BCL10 has been shown to be aided by another molecule, BCL3, in the human breast carcinoma cell line MCF7 [25] and the diffuse large B-cell lymphoma cell line Pfeiffer [30]. A small-scale yeast two-hybrid screen identified BCL3 as a potential binding partner of BCL10 in our NK tumour cell lines (data not shown). To further confirm the potential interaction between these two molecules, we enriched BCL10 from the crude protein lysates by immunoprecipitation and examined whether BCL3 is a binding partner of BCL10 by western blotting. As shown in Figure 6, the BCL10 antibody was able to

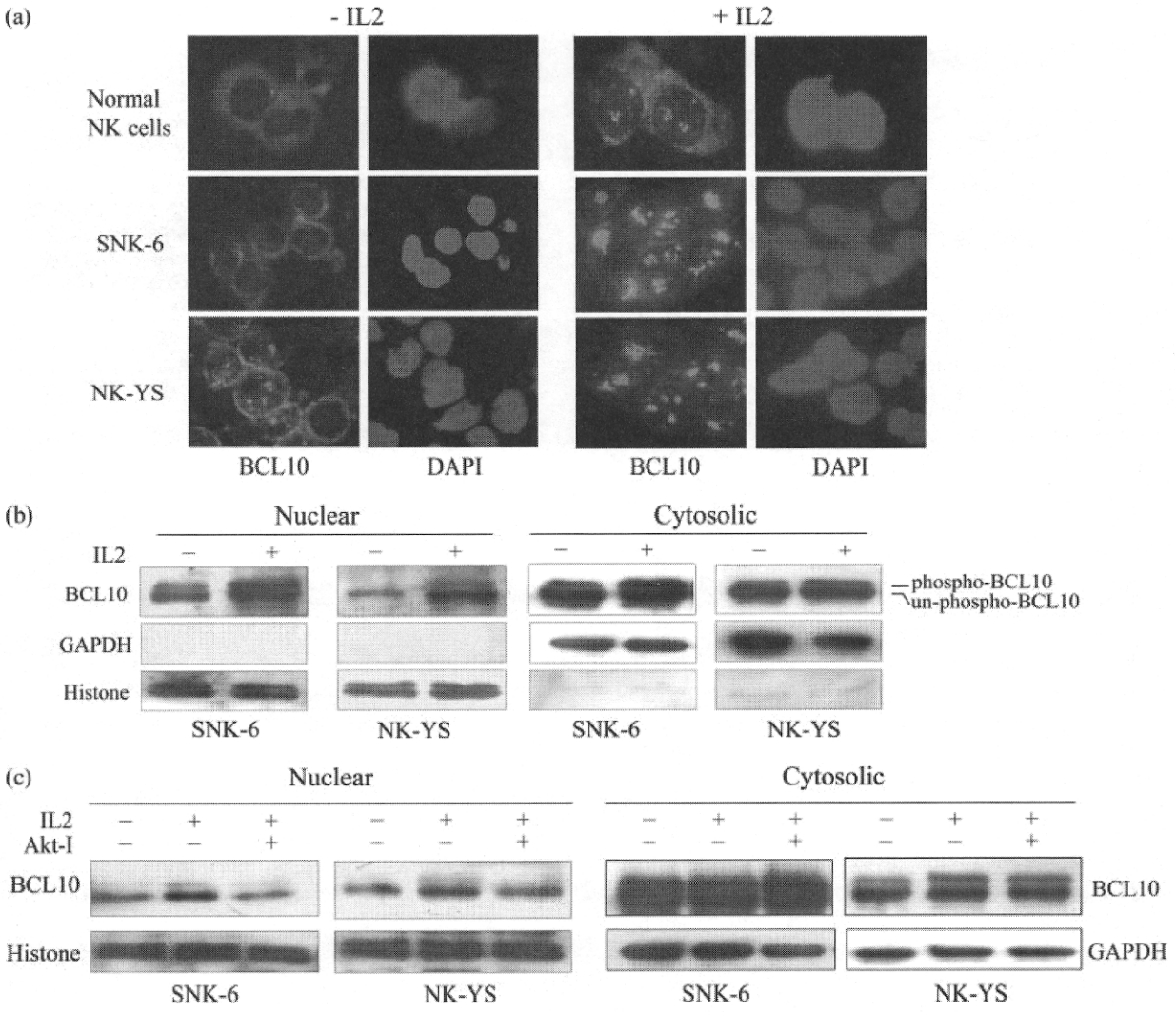

Figure 5. IL2 induces the nuclear translocation of BCL10 in normal and neoplastic NK cells. (a) Immunofluorescence micrographs of the NK-cell cytospin preparations. NK cells were cultured for 24 h in the presence or absence of IL2 (original magnification 400×). BCL10 was detected with a FITC-conjugated antibody (green) and the nuclei were stained with DAPI (blue). (b) Immunoblotting results for BCL10 in protein extracts from subcellular fractionation. GAPDH and histone served as the normalization controls for cytosolic and nuclear proteins, respectively. (c) Immunoblotting results for BCL10 in nuclear and cytosolic extracts from the NK cell lines. The combination of IL2 (300 U/ml) and Akt-I (10 μM) is specified in the figure. GAPDH and histone were used as loading controls for the cytosolic and nuclear extracts, respectively.

co-immunoprecipitate BCL3 in both SNK-6 and NK-YS cells, indicating that they form a complex in these IL2-activated NK cells.

IL2 induces BCL3 overexpression and translocation to the nucleus

We next investigated the molecular response of BCL3 following IL2 stimulation by examining the expression of BCL3 at both the transcriptional and the translational levels. IL2 induced increases in the mRNA and protein levels of BCL3 (Figures 7a and 7b). This effect was again blocked by Akt-I, showing the involvement of the PI3K/Akt pathway (Figure 7c). We next examined whether IL2 could induce the nuclear translocation of BCL3. Western blot analysis showed that more BCL3 was present in both the nuclear and the cytosolic fractions of NK cell lines when they were grown in the presence of IL2 (Figure 7d). Treatment with Akt-I reduced the amount of nuclear and cytosolic BCL3, suggesting that BCL3 expression was affected. Thus, the decrease in the level of nuclear BCL3 must be a result of the down-regulation of BCL3 expression caused by Akt-I.

BCL3 plays a role in the subcellular localization of BCL10

To clarify further the role of BCL3 in the nuclear transfer of BCL10, we used shRNA to suppress the expression of BCL3 and evaluated the subsequent effects on BCL10 subcellular localization. Two sequences targeting *BCL3* mRNA were examined and sequence B was selected to knock down BCL3 expression in

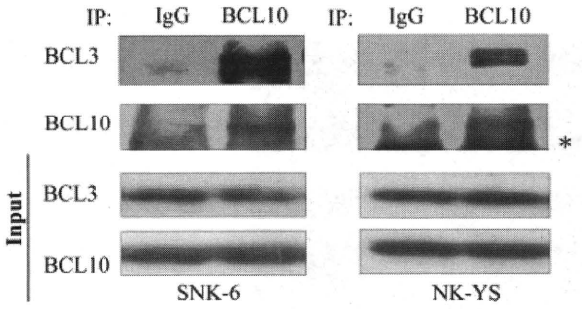

Figure 6. Co-immunoprecipitation of BCL3 with BCL10. An interaction between BCL3 and BCL10 was demonstrated by immunoprecipitation. Whole cell extracts were immunoprecipitated with an anti-BCL10 antibody or isotype-matched IgG (control). The purified product was examined with antibodies against BCL3 and BCL10 by immunoblotting. The asterisk indicates non-specific bands from the immunoglobulin light chains. The 'Input' control shows that the same amount of protein was used for immunoprecipitation.

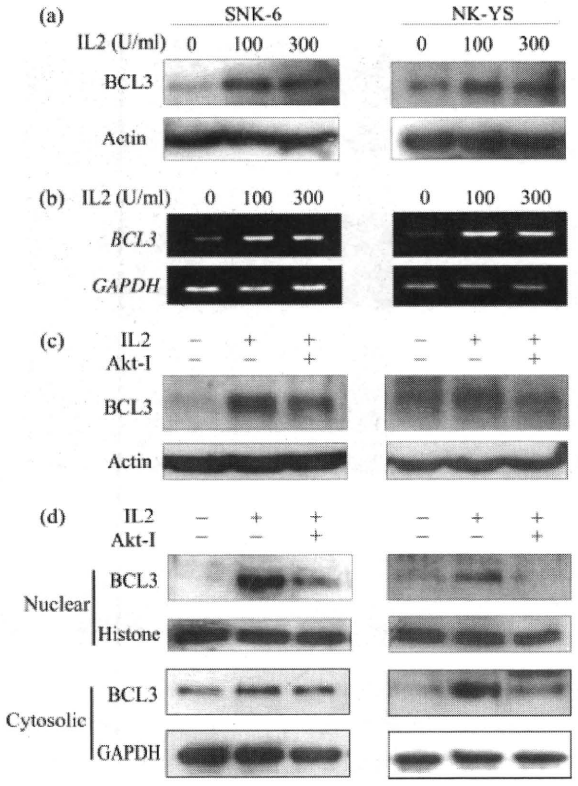

Figure 7. IL2 increases the transcript and protein levels of BCL3. Immunoblotting (a) and RT-PCR results (b) for BCL3 expression in NK cell lines treated with different concentrations of IL2. Actin and GAPDH were used as the normalization controls for a and b, respectively. (c) Immunoblotting results for BCL3 expression. Actin served as the normalization control. (d) Change in the amount of BCL3 in the nuclear and cytosolic extracts. GAPDH and histone were used as loading controls for the cytosolic and nuclear extracts, respectively. For c and d, the combination of IL2 (300 U/ml) or Akt-I (10 μM) is specified in the figure.

subsequent experiments (Figure 8a). After infection with the retrovirus carrying the shRNA sequence, SNK-6 cells showed a decrease in BCL3 expression in both the nuclear and the cytosolic extracts. Notably, BCL10 expression decreased along with BCL3 in the nuclear fractions, while cytosolic BCL10 expression remained unchanged (Figure 8b). To identify whether *de novo* protein synthesis is necessary for the translocation, we treated the cells with cycloheximide (CHX), a protein synthesis inhibitor, before stimulation with IL2. This treatment blocked the presence of BCL10 and BCL3 in the nuclear fractions and BCL3 in the cytosolic fractions (Figure 8c). There was a considerable amount of BCL10 in the cytosolic fractions, however, as it is more stable than BCL3. This result suggests that *de novo* synthesis of both BCL10 and BCL3 is necessary for their appearance in the nucleus in response to IL2.

Discussion

Cytokine receptor-induced lymphocyte activation often plays a role in the inflammatory and immune responses that occasionally give rise to lymphomagenesis [31,32]. In low-grade MALT lymphoma, the growth of tumour cells is maintained by stimulating signals from pro-inflammatory cytokines produced during chronic gastritis with persistent infection by *Helicobacter pylori*. Antibiotics that kill *H. pylori* block lymphocyte activation signalling, curing the gastritis and even the MALT lymphoma itself [33,34]. Similarly, ENKL is a lymphoid malignancy associated with Epstein–Barr virus infection [35]. A latent viral product such as LMP1 can up-regulate the expression of different cytokines, including interferon and IL10 [36,37]. Moreover, NK lymphoma cells are functionally active in a cytolytic manner and are characterized by constitutive activation of NF-κB [2], suggesting that cytokine-driven lymphocyte activation is essential for the development of NK cell lymphoma.

With regard to the use of IL2 as a model to study cytokine-driven NF-κB activation, we believe that IL2 is likely among the few cytokines that promote tumourigenesis in NK cell malignancies. It is required to maintain NK cell proliferation *in vitro*, and primary NK cells in human lymph nodes are dependent on T-cell-derived IL2 for cytotoxicity, in addition to viability and proliferation [19]. ENKLs are neoplasms with a cytotoxic NK phenotype [2]. ENKL cells do not express IL2 [38], but reactive T cells in the tumour micro-environment are likely a major source of IL2. Tumour-infiltrating T cells are prevalent in ENKL specimens [39–41] and frequently, they are the major cell population within the primary site and metastases of ENKL [41]. Conceivably IL-2 can be provided by activated T cells *in vivo* in ENKLs.

In the present study, we demonstrated that IL2 triggers NF-κB activation through the Akt pathway. Extensive studies have shown that BCL10 is a key mediator of NF-κB signalling in lymphocytes [42,43]. Along with its conventional role in antigen receptor signalling, recent studies have shown the involvement of BCL10 in mediating NF-κB signalling downstream of G protein-coupled receptors and Toll-like receptors

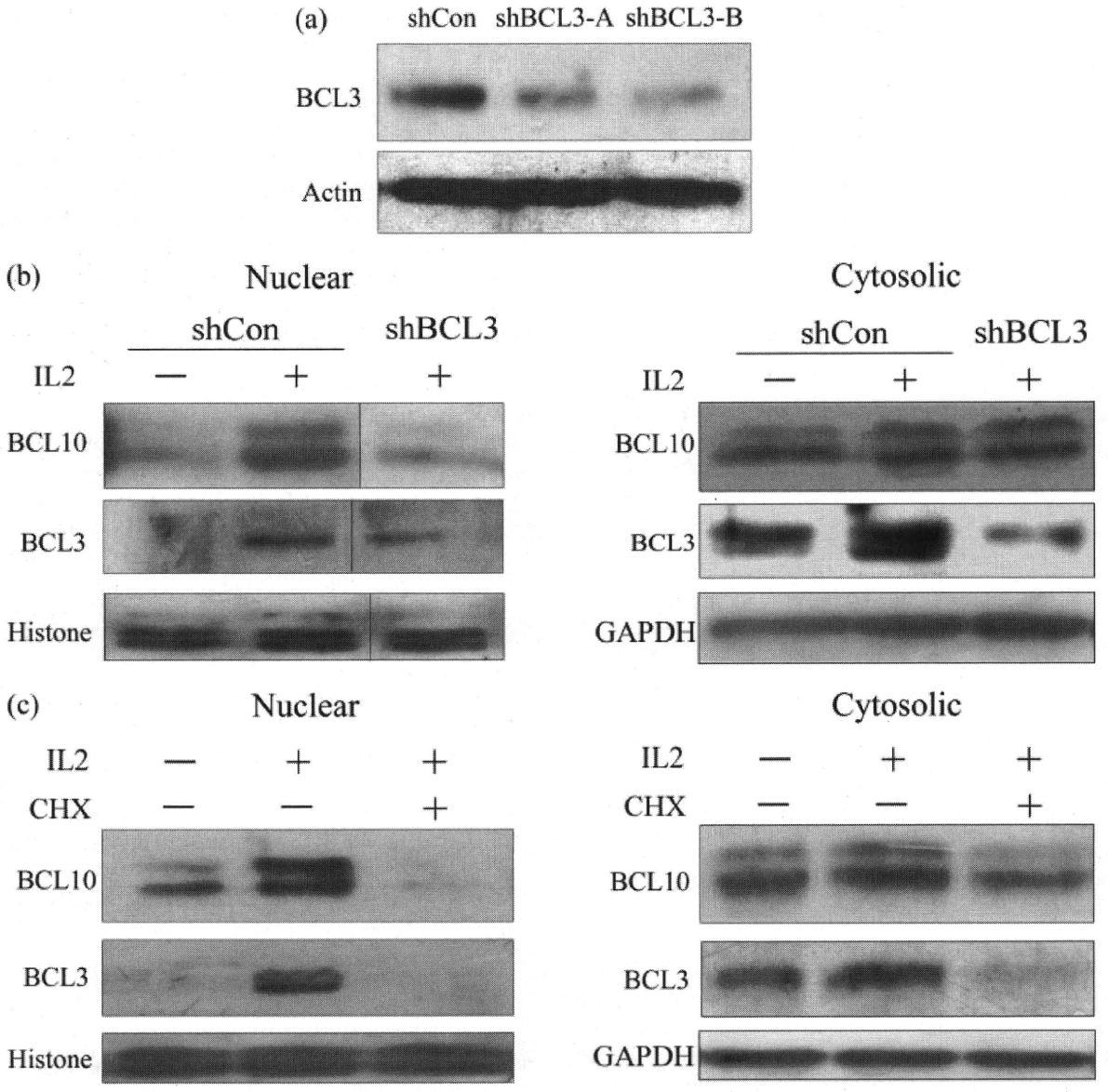

Figure 8. Knockdown of BCL3 expression by shRNA or CHX affects the nuclear localization of BCL10. (a) Immunoblotting results for BCL3 in SNK-6 cells. The expression of BCL3 was knocked down using two shRNA sequences. Actin served as the normalization control for immunoblotting. (b) Immunoblotting result for BCL10 and BCL3 in the nuclear and cytosolic extracts. shRNA-transduced SNK-6 cells were grown in the presence or absence of IL2 (300 U/ml) before cellular fractionation. (c) Immunoblotting results for BCL10 and BCL3 in the nuclear and cytosolic extracts. NK-YS cells were treated with IL2 in the presence or absence of 80 μg/ml CHX for 24 h before cellular fractionation. For b and c, GAPDH and histone were used as loading controls for the cytosolic and nuclear extracts, respectively.

[44,45]. Here we have provided evidence that BCL10 also participates in cytokine receptor-induced NF-κB signalling. Similar to the role of PKC in antigen receptor signalling, Akt is the kinase responsible for signal transduction via the IL2 receptor. Downstream of these kinases, BCL10 acts as a conductor to orchestrate NF-κB activation signalling, which is linked to different receptors, suggesting that BCL10 is a crucial adaptor in immune cells.

The nuclear localization of BCL10 is a recurrent phenomenon associated with MALT lymphoma and ENKL [4,46], indicating that aberrant nuclear BCL10 expression might play a role in the development of these diseases. Moreover, a distinct group of MALT lymphoma patients have shorter failure-free survival associated with the presence of nuclear BCL10 [47]. Thus, the identification of mechanisms that regulate the subcellular localization of BCL10 may be beneficial. An earlier report indicated that BCL3, a member of the IκB family, may be a binding partner of BCL10 in the nucleus [25]. That study focused on the human breast carcinoma cell line MCF7, however, raising concerns that the findings may not be representative of the actions of BCL3 in lymphoid cells. Kuo *et al* recently reported that B-cell activating factor (BAFF), a tumour necrosis factor-related cytokine, induces the nuclear transfer of BCL10 via BCL3 in the B-cell lymphoma cell line Pfeiffer [30]. Here we have described a similar

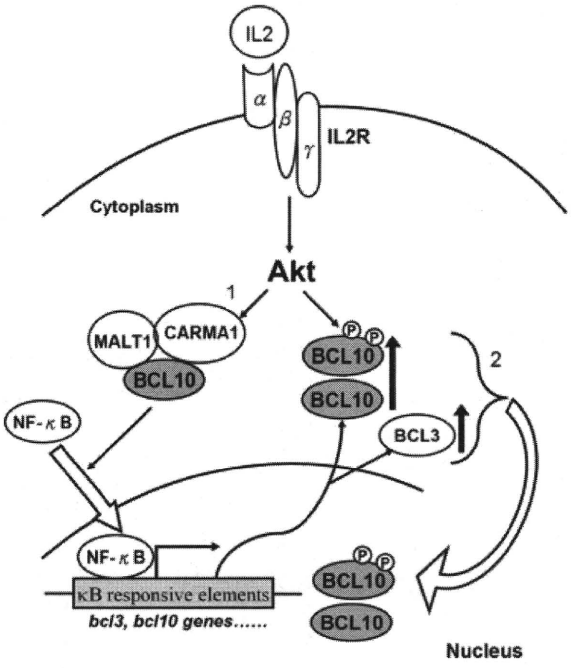

Figure 9. Schematic diagram of BCL3/BCL10-mediated NF-κB signalling modulation in ENKL. (1) Engagement of the IL2 receptor with IL2 activates the canonical NF-κB signalling pathway via Akt and this leads to a global increase in the expression of NF-κB-responsive genes. BCL3 and BCL10 expression are up-regulated and more protein appears in the cytosol. A circuit of BCL10 overexpression forms and promotes NF-κB activation. (2) On the other hand, BCL3 binds to BCL10 and facilitates BCL10 nuclear translocation. The level of BCL10 decreases in the cytosol and formation of the CARMA1–BCL10–MALT1 signalosome is inhibited. This negative feedback modulates NF-κB signalling.

scenario, demonstrating that IL2 induces the nuclear localization of both BCL3 and BCL10 in ENKL cells. This study provides an underlying mechanism for the nuclear translocation of BCL10 and more significantly, we have identified the essential role of BCL10 that connects IL2 receptor signalling with NF-κB activation. Because IL2 is a cytokine that plays a crucial role in the proliferation and development of T, B, and NK cells [48], the identification of BCL10 in the NK-cell activation signalling pathway that links the IL2 receptor with NF-κB activation is of great significance.

In Figure 8 we show that BCL10 nuclear translocation is dependent on the availability of BCL3. When BCL3 was silenced by RNA interference, BCL10 nuclear translocation was suppressed accordingly. Furthermore, when overall protein translation was suppressed by CHX, the nuclear transfer of BCL10 was diminished. This indicates that the nuclear translocation of BCL3 and BCL10 is dependent on the availability of new proteins, which are continuously generated. Overexpression of BCL3 may promote the nuclear translocation of BCL10. On the other hand, BCL3 is a member of the IκB family that does not act on the IKK complex. It plays a role as an NF-κB co-activator in the nucleus and is believed to be oncogenic [49]. Overexpression of BCL3 has been detected in multiple types of leukaemias and lymphomas [50]. Besides its role as a BCL10 binding partner, BCL3 has other roles that may also contribute to tumourigenesis.

As shown in Figure 9, up-regulation of BCL10 expression may occur via NF-κB binding to its potential 5′ UTR [25], which will transduce more activating signals through the amplification loop from BCL10 to NF-κB. The excess amount of BCL10 may exceed the number of MALT1 molecules, allowing BCL10 to escape cytosolic retention by MALT1 and enter into the nucleus [8,51]. Up-regulation of BCL3 would allow it to carry more BCL10 into the nucleus. If more BCL10 translocates into nucleus, the excess of BCL10 in the cytosol—where the CARMA1–BCL10–MALT1 signalosome is formed and plays a role in NF-κB signalling—would be reduced. Therefore, nuclear translocation of BCL10 is a result of NF-κB activation and in turn, it is used to modulate NF-κB signalling. A recent report also suggested that BCL10 in the nucleus is subject to degradation via the proteasome [52]. Thus, the nuclear translocation of BCL10 could represent a feedback mechanism that modulates 'exaggerated' NF-κB signalling. Other functions of nuclear BCL10, however, remain to be determined.

In summary, we have identified a critical role for BCL10 in cytokine receptor-induced NF-κB signalling, which results in NK cell activation. We also determined the underlying mechanism of the nuclear translocation of BCL10, which was found to be associated with constitutive NF-κB activation. Given that knockdown of BCL10 by shBCL10 suppressed the IL2-induced entry of SNK-6 cells into the G2/M phase of the cell cycle (an anti-proliferative effect), silencing of BCL10 might be a potential therapeutic option to kill ENKL tumour cells.

Acknowledgment

This study was supported by the General Research Fund (GRF) of the Research Grants Council of Hong Kong, China (HKU 7583/54M to GS and RHS).

References

1. Jaffe E, Chan J, Su I, Frizzera G, Mori S, Feller AC, *et al.* Report of the workshop on nasal and related extranodal angiocentric T/natural killer cell lymphomas. Definitions, differential diagnosis, and epidemiology. *Am J Surg Pathol* 1996; **20**: 103–111.
2. Chiang A, Chan A, Srivastava G, Ho F. Nasal NK/T-cell lymphomas are derived from Epstein–Barr virus-infected cytotoxic lymphocytes of both NK- and T-cell lineage. *Int J Cancer* 1997; **73**: 332–338.
3. Kaneko T, Fukuda J, Yoshihara T, Zheng H, Mori S, Mizoguchi H, *et al.* Nasal natural killer (NK) cell lymphoma: report of a case with activated NK cells containing Epstein–Barr virus and expressing CD21 antigen, and comparative studies of their phenotype and cytotoxicity with normal NK cells. *Br J Haematol* 1995; **91**: 355–361.
4. Shen L, Liang ACT, Lu L, Au WY, Wong KY, Tin PC, *et al.* Aberrant BCL10 nuclear expression in nasal NK/T-cell lymphoma. *Blood* 2003; **102**: 1553–1554.

5. Willis TG, Jadayel DM, Du MQ, Peng H, Perry AR, Abdul-Rauf M, *et al.* Bcl10 is involved in t(1;14)(p22;q32) of MALT B cell lymphoma and mutated in multiple tumor types. *Cell* 1999; **96**: 35–45.
6. Ye H, Dogan A, Karran L, Willis TG, Chen L, Wlodarska I, *et al.* BCL10 expression in normal and neoplastic lymphoid tissue. *Am J Pathol* 2000; **157**: 1147–1154.
7. Hu S, Du MQ, Park SM, Alcivar A, Qu L, Gupta S, *et al.* cIAP2 is a ubiquitin protein ligase for BCL10 and is dysregulated in mucosa-associated lymphoid tissue lymphomas. *J Clin Invest* 2006; **116**: 174–181.
8. Nakagawa M, Hosokawa Y, Yonezumi M, Izumiyama K, Suzuki R, Tsuzuki S, *et al.* MALT1 contains nuclear export signals and regulates cytoplasmic localization of BCL10. *Blood* 2005; **106**: 4210–4216.
9. Thome M. CARMA1, BCL10 and MALT1 in lymphocyte development and activation. *Nature Rev Immunol* 2004; **4**: 348–359.
10. Lucas PC, McAllister-Lucas LM, Nunez G. NF-κB signaling in lymphocytes: a new cast of characters. *J Cell Sci* 2004; **117**: 31–39.
11. Ruland J, Duncan GS, Elia A, Barrantes IB, Nguyen L, Plyte S, *et al.* Bcl10 is a positive regulator of antigen receptor-induced activation of NF-κB and neural tube closure. *Cell* 2001; **104**: 33–42.
12. Wegener E, Krappmann D. CARD–Bcl10–Malt1 signalosomes: missing link to NF-κB. *Sci STKE* 2007; **384**: pe21.
13. Malarkannan S, Regunathan J, Chu H, Kutlesa S, Chen Y, Zeng H, *et al.* Bcl10 plays a divergent role in NK cell-mediated cytotoxicity and cytokine generation. *J Immunol* 2007; **179**: 3752–3762.
14. Gross O, Grupp C, Steinberg C, Zimmermann S, Strasser D, Hannesschläger N, *et al.* Multiple ITAM-coupled NK-cell receptors engage the Bcl10/Malt1 complex via Carma1 for NF-κB and MAPK activation to selectively control cytokine production. *Blood* 2008; **112**: 2421–2428.
15. Cozen W, Gill P, Salam M, Nieters A, Masood R, Cockburn M, *et al.* Interleukin-2, interleukin-12, and interferon-gamma levels and risk of young adult Hodgkin lymphoma. *Blood* 2008; **111**: 3377–3382.
16. Chopra CG, Chitalkar LCP, Jaiprakash MGM. Cytokines: as useful prognostic markers in lymphoma cases. *Med J Armed Forces India* 2004; **60**: 45–49.
17. Su H, Orange J, Fast L, Chan A, Simpson S, Terhorst C, *et al.* IL-2-dependent NK cell responses discovered in virus-infected β_2-microglobulin-deficient mice. *J Immunol* 1994; **153**: 5674–5681.
18. Zhang Y, Nagata H, Ikeuchi T, Mukai H, Oyoshi MK, Demachi A, *et al.* Common cytological and cytogenetic features of Epstein–Barr virus (EBV)-positive natural killer (NK) cells and cell lines derived from patients with nasal T/NK-cell lymphomas, chronic active EBV infection and hydroa vacciniforme-like eruptions. *Br J Haematol* 2003; **121**: 805–814.
19. Fehniger T, Cooper M, Nuovo G, Cella M, Facchetti F, Colonna M, *et al.* $CD56^{bright}$ natural killer cells are present in human lymph nodes and are activated by T cell-derived IL-2: a potential new link between adaptive and innate immunity. *Blood* 2003; **101**: 3052–3057.
20. Zhou J, Zhang J, Lichtenheld MG, Meadows GG. A role for NF-κB activation in perforin expression of NK cells upon IL-2 receptor signaling. *J Immunol* 2002; **169**: 1319–1325.
21. Burchilla MA, Yanga J, Vanga KB, Farrar MA. Interleukin-2 receptor signaling in regulatory T cell development and homeostasis. *Immunol Lett* 2007; **114**: 1–8.
22. Jiang K, Zhong B, Ritchey C, Gilvary DL, Hong-Geller E, Wei S, *et al.* Regulation of Akt-dependent cell survival by Syk and Rac. *Blood* 2003; **101**: 236–244.
23. Narayan P, Holt B, Tosti R, Kane LP. CARMA1 is required for Akt-mediated NF-κB activation in T cells. *Mol Cell Biol* 2006; **26**: 2327–2336.
24. Kane LP, Shapiro VS, Stokoe D, Weiss A. Induction of NF-κB by the Akt/PKB kinase. *Curr Biol* 1999; **9**: 601–604.
25. Yeh PY, Kuo SH, Yeh KH, Chuang SE, Hsu CH, Chang WC, *et al.* A pathway for tumor necrosis factor-α-induced BCL10 nuclear translocation. BCL10 is up-regulated by NF-κB and phosphorylated by Akt1 and then complexes with BCL3 to enter the nucleus. *J Biol Chem* 2006; **281**: 167–175.
26. Matsuo Y, Drexler HG. Immunoprofiling of cell lines derived from natural killer-cell and natural killer-like T-cell leukemia–lymphoma. *Leuk Res* 2003; **27**: 935–945.
27. Hu Y, Qiao L, Wang S, Rong SB, Meuillet EJ, Berggren M, *et al.* 3-(Hydroxymethyl)-bearing phosphatidylinositol ether lipid analogues and carbonate surrogates block PI3-K, Akt, and cancer cell growth. *J Med Chem* 2000; **43**: 3045–3051.
28. Huang C, Bi E, Hu Y, Deng W, Tian Z, Dong C, *et al.* A novel NF-κB binding site controls human granzyme B gene transcription. *J Immunol* 2006; **176**: 4173–4181.
29. Yemelyanov A, Gasparian A, Lindholm P, Dang L, Pierce JW, Kisseljov F, *et al.* Effects of IKK inhibitor PS1145 on NF-κB function, proliferation, apoptosis and invasion activity in prostate carcinoma cells. *Oncogene* 2006; **25**: 387–398.
30. Kuo SH, Yeh PY, Chen LT, Wu MS, Lin CW, Yeh KH, *et al.* Overexpression of B cell-activating factor of TNF family (BAFF) is associated with *Helicobacter pylori*-independent growth of gastric diffuse large B-cell lymphoma with histologic evidence of MALT lymphoma. *Blood* 2008; **112**: 2927–2934.
31. Nacinović-Duletić A, Stifter S, Dvornik S, Skunca Z, Jonjić N. Correlation of serum IL-6, IL-8 and IL-10 levels with clinicopathological features and prognosis in patients with diffuse large B-cell lymphoma. *Int J Lab Haematol* 2008; **30**: 230–239.
32. Skinnider BF, Mak TW. The role of cytokines in classical Hodgkin lymphoma. *Blood* 2002; **99**: 4283–4297.
33. Dong G, Liu C, Ye H, Gong L, Zheng J, Li M, *et al.* BCL10 nuclear expression and t(11;18)(q21;q21) indicate nonresponsiveness to *Helicobacter pylori* eradication of Chinese primary gastric MALT lymphoma. *Int J Hematol* 2008; **88**: 516–523.
34. Yeh KH, Kuo SH, Chen LT, Mao TL, Doong SL, Wu MS, *et al.* Nuclear expression of BCL10 or nuclear factor-κB helps predict *Helicobacter pylori*-independent status of low-grade gastric mucosa-associated lymphoid tissue lymphomas with or without t(11;18)(q21;q21). *Blood* 2005; **106**: 1037–1041.
35. Isobe Y, Sugimoto K, Yang L, Tamayose K, Egashira M, Kaneko T, *et al.* Epstein–Barr virus infection of human natural killer cell lines and peripheral blood natural killer cells. *Cancer Res* 2004; **64**: 2167–2174.
36. Lambert S, Martinez O. Latent membrane protein 1 of EBV activates phosphatidylinositol 3-kinase to induce production of IL-10. *J Immunol* 2007; **179**: 8225–8234.
37. Najjar I, Baran-Marszak F, Clorennec CL, Laguillier C, Schischmanoff O, Youlyouz-Marfak I, *et al.* Latent membrane protein 1 regulates STAT1 through NF-κB-dependent interferon secretion in Epstein–Barr virus-immortalized B cells. *J Virol* 2005; **79**: 4936–4943.
38. Ho JW, Liang RH, Srivastava G. Differential cytokine expression in EBV positive peripheral T cell lymphomas. *Mol Pathol* 1999; **52**: 269–274.
39. Tao Q, Chiang AK, Srivastava G, Ho FC. TCR-CD56+CD2+ nasal lymphomas with membrane-localized CD3 positivity: are the CD3+ cells neoplastic or reactive? *Blood* 1995; **85**: 2993–2996.
40. Shen L, Liang AK, Liu WP, Li PD, Liang RH, Srivastava G. Expression of HLA class I, beta(2)-microglobulin, TAP1 and IL-10 in Epstein–Barr virus-associated nasal NK/T-cell lymphoma:

implications for tumor immune escape mechanism. *Int J Cancer* 2001; **92**: 692–696.
41. Falcão RP, Rizzatti EG, Saggioro FP, Garcia AB, Marinato AF, Rego EM. Flow cytometry characterization of leukemic phase of nasal NK/T-cell lymphoma in tumor biopsies and peripheral blood. *Haematologica* 2007; **92**: e24–e25.
42. Thome M, Tschopp J. TCR-induced NF-κB activation: a crucial role for Carma1, Bcl10 and MALT1. *Trends Immunol* 2003; **24**: 419–424.
43. Tian MT, Gonzalez G, Scheer B, DeFranco AL. Bcl10 can promote survival of antigen-stimulated B lymphocytes. *Blood* 2005; **106**: 2105–2112.
44. Hara H, Ishihara C, Takeuchi A, Imanishi T, Xue L, Morris SW, *et al*. The adaptor protein CARD9 is essential for the activation of myeloid cells through ITAM-associated and Toll-like receptors. *Nature Immunol* 2007; **8**: 619–629.
45. Wang D, You Y, Lin PC, Xue L, Morris SW, Zeng H, *et al*. Bcl10 plays a critical role in NF-κB activation induced by G protein-coupled receptors. *Proc Natl Acad Sci U S A* 2007; **104**: 145–150.
46. Isaacson P, Du M. MALT lymphoma: from morphology to molecules. *Nature Rev Cancer* 2004; **4**: 644–653.
47. Franco R, Camacho FI, Caleo A, Staibano S, Bifano D, Renzo AD, *et al*. Nuclear bcl10 expression characterizes a group of ocular adnexa MALT lymphomas with shorter failure-free survival. *Mod Pathol* 2006; **19**: 1055–1067.
48. Mak TW, Saunders ME. *The Immune Response: Basic and Clinical Principles*. Elsevier: Boston, 2006; 477–479.
49. Franzoso G, Bours V, Azarenko V, Park S, Tomita-Yamaguchi M, Kanno T, *et al*. The oncoprotein Bcl-3 can facilitate NF-κB-mediated transactivation by removing inhibiting p50 homodimers from select κB sites. *EMBO J* 1993; **12**: 3893–3901.
50. McKeithan TW, Takimoto GS, Ohno H, Bjorling VS, Morgan R, Hecht BK, *et al*. BCL3 rearrangements and t(14;19) in chronic lymphocytic leukemia and other B-cell malignancies: a molecular and cytogenetic study *Genes Chromosomes Cancer* 1997; **20**: 64–72.
51. Ye H, Gesk S, Martin-Subero J, Nader A, Du M, Siebert R. BCL10 gene amplification associated with strong nuclear BCL10 expression in a diffuse large B cell lymphoma with IGH–BCL2 fusion. *Haematologica* 2006; **91**: e81–82.
52. Lobry C, Lopez T, Israël A, Weil R. Negative feedback loop in T cell activation through IκB kinase-induced phosphorylation and degradation of Bcl10. *Proc Natl Acad Sci U S A* 2007; **104**: 908–913.

SUPPORTING INFORMATION ON THE INTERNET

The following supporting information may be found in the online version of this article.

Table S1. List of the antibodies used in the study.

Table S2. Sequences of the primers used for semi-quantitative RT-PCR in the study.

Table S3. Sequences of the primers used for quantitative real-time RT-PCR in the study.

Table S4. shRNA sequences for BCL10 and BCL3 used in the study.

Immunology
The Journal of cells, molecules, systems and technologies
British Society for immunology

IMMUNOLOGY ORIGINAL ARTICLE

Ex vivo expanded cord blood CD4 T lymphocytes exhibit a distinct expression profile of cytokine-related genes from those of peripheral blood origin

Yoshitaka Miyagawa,[1] Nobutaka Kiyokawa,[1] Nakaba Ochiai,[2,3] Ken-Ichi Imadome,[4] Yasuomi Horiuchi,[1] Keiko Onda,[1] Misako Yajima,[4] Hiroyuki Nakamura,[4] Yohko U. Katagiri,[1] Hajime Okita,[1] Tomohiro Morio,[2,5] Norio Shimizu,[2,6] Junichiro Fujimoto[7] and Shigeyoshi Fujiwara,[4]

[1]*Department of Developmental Biology, National Research Institute for Child Health and Development, Setagaya-ku,* [2]*Center for Cell Therapy, Tokyo Medical and Dental University Medical Hospital, Bunkyo-ku, Tokyo,* [3]*Lymphotec Inc., Koto-ku, Tokyo,* [4]*Department of Infectious Diseases, National Research Institute for Child Health and Development, Setagaya-ku, Tokyo,* [5]*Department of Pediatrics and Developmental Biology, Graduate School of Medicine, Tokyo Medical and Dental University, Bunkyo-ku, Tokyo,* [6]*Department of Virology, Division of Medical Science, Medical Research Institute, Tokyo Medical and Dental University, Bunkyo-ku, Tokyo, and* [7]*Vice Director General, National Research Institute for Child Health and Development, Setagaya-ku, Tokyo, Japan*

Summary

With an increase in the importance of umbilical cord blood (CB) as an alternative source of haematopoietic progenitors for allogenic transplantation, donor lymphocyte infusion (DLI) with donor CB-derived activated $CD4^+$ T cells in the unrelated CB transplantation setting is expected to be of increased usefulness as a direct approach for improving post-transplant immune function. To clarify the characteristics of activated $CD4^+$ T cells derived from CB, we investigated their mRNA expression profiles and compared them with those of peripheral blood (PB)-derived activated $CD4^+$ T cells. Based on the results of a DNA microarray analysis and quantitative real-time reverse transcriptase–polymerase chain reaction (RT-PCR), a relatively high level of forkhead box protein 3 (Foxp3) gene expression and a relatively low level of interleukin (IL)-17 gene expression were revealed to be significant features of the gene expression profile of CB-derived activated $CD4^+$ T cells. Flow cytometric analysis further revealed protein expression of Foxp3 in a portion of CB-derived activated $CD4^+$ T cells. The low level of retinoic acid receptor-related orphan receptor γ isoform t (RORγt) gene expression in CB-derived activated $CD4^+$ T cells was speculated to be responsible for the low level of IL-17 gene expression. Our data indicate a difference in gene expression between $CD4^+$ T cells from CB and those from PB. The findings of Foxp3 expression, a characteristic of regulatory T cells, and a low level of IL-17 gene expression suggest that CB-derived $CD4^+$ T cells may be a more appropriate source for DLI.

Keywords: CD4; cord blood; donor lymphocyte infusion; forkhead box protein 3; interleukin 17; T cell

doi:10.1111/j.1365-2567.2009.03122.x
Received 1 September 2008; revised 30 March 2009; accepted 15 April 2009.
Correspondence: N. Kiyokawa, MD, PhD, Department of Developmental Biology, National Research Institute for Child Health and Development, 2-10-1, Okura, Setagaya-ku, Tokyo 157-8535, Japan.
Email: nkiyokawa@nch.go.jp
Senior author: Nobutaka Kiyokawa

Abbreviations: BIM, BCL2-like 11; CB, cord blood; CTLA-4, cytotoxic T-lymphocyte antigen-4; CDKN, cyclin-dependent kinase inhibitor; DLI, donor lymphocyte infusion; Foxp3, forkhead box protein 3; GAPDH, glyceraldehyde-3-phosphate dehydrogenase; GM-CSF, granulocyte–macrophage colony-stimulating factor; GVHD, graft-versus-host disease; GVL, graft-versus-leukaemia; HSCT, haematopoietic stem cell transplantation; ICOS, inducible T-cell co-stimulator; IFNG, interferon γ; IL, interleukin; PB, peripheral blood; RORγt, retinoic acid receptor-related orphan receptor γ isoform t; RT, reverse transcriptase; TCR, T-cell receptor; Th, T helper cell; Treg, regulatory T cell.

Introduction

Donor lymphocyte infusion (DLI) is a direct and useful approach for improving post-transplant immune function. DLI has been shown to exert a graft-versus-leukaemia (GVL) effect and has emerged as an effective strategy for the treatment of patients with leukaemia, especially chronic myelogenous leukaemia, who have relapsed after unrelated haematopoietic stem cell transplantation (HSCT).[1] In addition, DLI has been successfully used for some life-threatening viral infections, including Epstein–Barr virus and cytomegalovirus infections after HSCT.[2]

Although DLI frequently results in significant acute and/or chronic graft-versus-host disease (GVHD), several groups have demonstrated that depletion of CD8 T cells from DLIs efficiently reduces the incidence and severity of GVHD while maintaining GVL activity.[3,4] Therefore, selective CD4 DLI is expected to provide an effective and low-toxicity therapeutic strategy for improving post-transplant immune function. Actually, selective CD4 DLI based on a recently established method for *ex vivo* T-cell expansion using anti-CD3 monoclonal antibody and interleukin (IL)-2 is now becoming established as a routine therapeutic means of resolving post-transplant immunological problems in Japan.[5]

The importance of umbilical cord blood (CB) as an alternative source of haematopoietic progenitors for allogenic transplantation, mainly in patients lacking a human leucocyte antigen (HLA)-matched marrow donor, has increased in recent years. Because of the naïve nature of CB lymphocytes, the incidence and severity of GVHD are reduced in comparison with the allogenic transplant setting. In addition, CB is rich in primitive $CD16^-$ $CD56^+$ natural killer (NK) cells, which possess significant proliferative and cytotoxic capacities, and so have a substantial GVL effect.[6]

In contrast, a major disadvantage of CB transplantation is the low yield of stem cells, resulting in higher rates of engraftment failure and slower engraftment compared with bone marrow transplantation. In addition, it was generally thought to be difficult to perform DLI after CB transplantation using donor peripheral blood (PB), with the exception of transplantations from siblings. However, the above-described method for the *ex vivo* expansion of activated T cells can produce a sufficient amount of cells for therapy using the CB cell residues in an infused bag, which has solved this problem and made it possible to perform DLI with donor CB-derived activated $CD4^+$ T cells in the unrelated CB transplantation setting.[5] It has also been reported that CB-derived T cells can be expanded *ex vivo* while retaining the naïve and/or central memory phenotype and polyclonal T-cell receptor (TCR) diversity,[7] and thus potential utilization for adoptive cellular immunotherapy post-CB transplantation has been suggested.[8]

There are functional differences between CB and PB lymphocytes, although the details remain unclear. In an attempt to clarify the differences in characteristics between activated $CD4^+$ T cells derived from CB and those derived from PB, we investigated gene expression profiles. In this paper we present evidence that CB-derived $CD4^+$ T cells are distinct from PB-derived $CD4^+$ T cells in terms of gene expression.

Materials and methods

Cell culture and preparation

CB was distributed by the Tokyo Cord Blood Bank (Tokyo, Japan). The CB was originally collected and stored for stem cell transplantation. Stocks that were inappropriate for transplantation because they contained too few cells were distributed for research use with informed consent, with the permission of the ethics committee of the bank. In addition, all of the experiments in this study using distributed CB were performed with the approval of the local ethics committee. The mononuclear cells were isolated by Ficoll-Paque centrifugation and cultured in the presence of an anti-CD3 monoclonal antibody and interleukin (IL)-2 using TLY Culture Kit 25 (Lymphotec Inc., Tokyo, Japan) as described previously.[5] Although several different methods for T-cell stimulation have been reported, this method is currently being used clinically in Japan. Thus we selected this method in this study. After 14 days of culture, $CD4^+$ cells were isolated using a magnetic-activated cell sorting (MACS) system (Miltenyi Biotec, Bergisch Gladbach, Germany) according to the manufacturer's instructions. As a control, mononuclear cells isolated from the peripheral blood of healthy volunteers were similar examined.

Polymerase chain reaction (PCR)

Total RNA was extracted from cells using an RNeasy kit (Qiagen, Valencia, CA) and reverse-transcribed using a First-Strand cDNA synthesis kit (GE Healthcare Bio-Science Corp., Little Chalfont, Buckinghamshire, UK) according to the manufacturer's instructions. Using cDNA synthesized from 150 ng of total RNA as a template for one amplification, real-time reverse transcriptase (RT)-PCR was performed using SYBR® Green PCR master mix, TaqMan® Universal PCR master mix and TaqMan® gene expression assays (Applied Biosystems, Foster City, CA), and an inventoried assay carried out on an ABI PRISM® 7900HT sequence detection system (Applied Biosystems) according to the instructions provided. Either the glyceraldehyde-3-phosphate dehydrogenase (GAPDH) gene or the β-actin gene was used as an internal control for normalization. The sequences of gene-specific primers for real-time RT-PCR are listed in Table 1.

DNA microarray analysis

The microarray analysis was performed as previously described.[9] Total RNA isolated from cells was reverse-

